ARMY RESEARCH LABORATORY

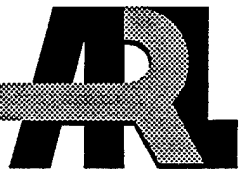

Thermal Radiation Transmission Through Composite Material

Richard B. Loucks

ARL-TR-784 June 1995

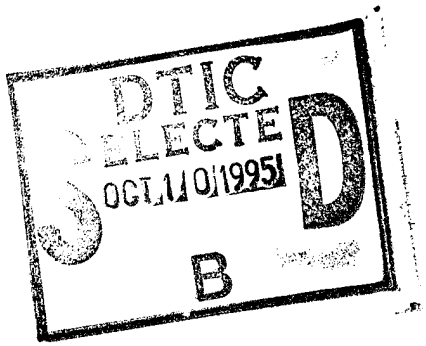

19951005 009

APPROVED FOR PUBLIC RELEASE; DISTRIBUTION IS UNLIMITED.

DTIC QUALITY INSPECTED 5

NOTICES

Destroy this report when it is no longer needed. DO NOT return it to the originator.

Additional copies of this report may be obtained from the National Technical Information Service, U.S. Department of Commerce, 5285 Port Royal Road, Springfield, VA 22161.

The findings of this report are not to be construed as an official Department of the Army position, unless so designated by other authorized documents.

The use of trade names or manufacturers' names in this report does not constitute endorsement of any commercial product.

REPORT DOCUMENTATION PAGE

Form Approved
OMB No. 0704-0188

Public reporting burden for this collection of information is estimated to average 1 hour per response, including the time for reviewing instructions, searching existing data sources, gathering and maintaining the data needed, and completing and reviewing the collection of information. Send comments regarding this burden estimate or any other aspect of this collection of information, including suggestions for reducing this burden, to Washington Headquarters Services, Directorate for Information Operations and Reports, 1215 Jefferson Davis Highway, Suite 1204, Arlington, VA 22202-4302, and to the Office of Management and Budget, Paperwork Reduction Project (0704-0188), Washington, DC 20503.

1. AGENCY USE ONLY *(Leave blank)*	2. REPORT DATE	3. REPORT TYPE AND DATES COVERED
	June 1995	Final, June 1994 - July 1994

4. TITLE AND SUBTITLE
Thermal Radiation Transmission Through Composite Material

5. FUNDING NUMBERS
4G061-405-U2

6. AUTHOR(S)
Richard B. Loucks

7. PERFORMING ORGANIZATION NAME(S) AND ADDRESS(ES)
U.S. Army Research Laboratory
ATTN: AMSRL-WT-NC
Aberdeen Proving Ground, MD 21005-5066

8. PERFORMING ORGANIZATION REPORT NUMBER
ARL-TR-784

9. SPONSORING / MONITORING AGENCY NAME(S) AND ADDRESS(ES)

10. SPONSORING / MONITORING AGENCY REPORT NUMBER

11. SUPPLEMENTARY NOTES

12a. DISTRIBUTION / AVAILABILITY STATEMENT
Approved for public release; distribution is unlimited

12b. DISTRIBUTION CODE

13. ABSTRACT *(Maximum 200 words)*

On 10 June 1993, the Defense Nuclear Agency (DNA) Field Command at White Sands Missile Range conducted a Thermal Radiation Simulator (TRS) test for the Naval Surface Warfare Center (NSWC) during project MINOR UNCLE. The NSWC was interested in measuring the radiant thermal energy absorbed by a fiberglass panel during a simulated nuclear weapon event. The resultant thermocouple data showed an unusual initial high-temperature rise and fall, followed by the expected conductive heating. The initial transient was theorized to be the result of thermal radiation transmitted through the panel. To investigate this theory, NSWC prepared several more panels of different thicknesses, preinstrumented with thermocouples and strain gages for testing with a U.S. Army Research Laboratory (ARL) TRS. ARL also provided additional instrumentation to measure thermal radiation on the front surface as well as behind the panel. The results showed that there was direct heating of the rear of the composite panel by thermal radiation. The quantity of heat transmission through the panel and the point of ignition of the front surface of the panel were determined. Smoke and charring of the front surface protected the panel from further heating and possible destruction.

14. SUBJECT TERMS	15. NUMBER OF PAGES
composite material, heat transfer, thermal radiation, nuclear explosion simulation	68
	16. PRICE CODE

17. SECURITY CLASSIFICATION OF REPORT	18. SECURITY CLASSIFICATION OF THIS PAGE	19. SECURITY CLASSIFICATION OF ABSTRACT	20. LIMITATION OF ABSTRACT
UNCLASSIFIED	UNCLASSIFIED	UNCLASSIFIED	UL

Intentionally left blank

ACKNOWLEDGMENTS

I would like to express my sincere appreciation to the following people for their support during these experiments. I am indebted to Pete Muller and Rick Thane for all their help with the experiments (without them, I do not really believe this experiment would have had a chance of happening); Larry Vande Kieft, for asking about the TRS and its abilities (had he not been curious about it, this work would have never been done); Bob Persch and Matt Rupalt, for having the problem and letting me try my theory out on some of their spare panels; Bud Raley, for encouraging me to pursue a "blue sky" idea, without it being in the branch annual plan; and finally, to Rich Lottero, for allowing this work to happen.

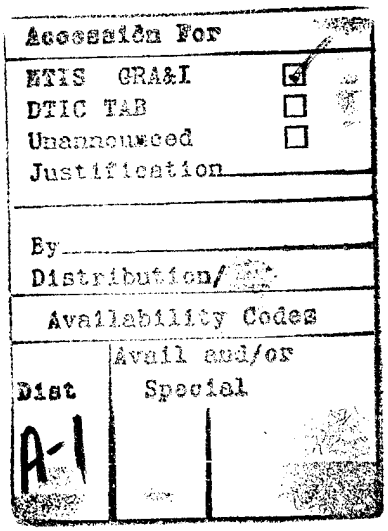

Intentionally Left Blank

TABLE OF CONTENTS

Page

ACKNOWLEDGMENTS iii

LIST OF FIGURES vii

LIST OF TABLES ix

1. INTRODUCTION 1

2. COMPOSITE PANEL EXPERIMENT 3

2.1 Thermal Radiation Simulator 4
2.1.1 TRS Compared to Nuclear Weapon Thermal Radiation. 5
2.1.2 TRS Simulation Profile. 8
2.2 Experiment Setup 11
2.2.1 Instrumentation 11
2.2.2 Experiment Setup and Process 14
2.3 Post Experiment Process 16

3. DATA ANALYSIS 17

3.1 TRS Data 18
3.2 Thermocouple and Strain Gage Data. 20
3.2.1 Fourier Transform Analysis. 21
3.2.2 Forcing Influence Extraction From the Data. 23

4. RESULTS 26

4.1 Thermal Effects Due to Different Mounting Methods. 26
4.2 Thermal Radiation Transmission 28
4.3 Smoke Generation and Protection. 29

5. CONCLUSIONS 30

6. REFERENCES 31

APPENDIX A: PARABOLIC INTERPOLATION OF DATA 33

APPENDIX B: PLOTS OF DATA. 39

APPENDIX C: CONTOUR PLOTS OF TRS DATA 51

DISTRIBUTION LIST 55

Intentionally left blank

LIST OF FIGURES

Figure		Page
1.	NSWC composite radome data.	2
2.	TRS unit as a free field source.	4
3.	ARL TRS thermal simulation profile.	5
4.	Nuclear thermal pulse profile, relative scale.	5
5.	2.44-m probative tube and TRS showing calorimeter array.	8
6.	Contour plot of isoradiance at 100 cm from center.	9
7.	Pre-experiment contour plots at 60 cm.	10
8.	Composite panel with sensors mounted on back.	12
9.	Controller and MEGADAC.	12
10.	Gardon-type gage for flux measurement.	13
11.	Composite panel on calorimeter array frame.	14
12.	TRS in test section.	16
13.	Thermal radiation data for each experiment at channel 9.	19
15.	Sensor data from Channel 12 and 13, TRS-7-94.	20
16.	TRS-9-94, calorimeter closest to composite panel.	21
17.	Magnitude of Fourier transform of thermocouple data and TRS data	22
18.	Obtaining a curve from data.	23
19.	Initial transient isolated from conduction data set.	24
21.	Compensated transducer signal.	25
22.	Comparison of normalized signal	25
23.	Comparison of thermal radiation effect on each sensor.	27
24.	Thermal radiation transmission, TRS-10-94.	28
25.	Thermal radiation transmission, TRS-11-94.	29
A-1.	Area of consideration in 2.44-m shock tube mock-up.	34
A-2.	Thermal mapping of isoradiance, linear connection.	37
B-1.	TRS data from TRS-7-94	40
B-2.	Sensor data, TRS-7-94	41
B-3.	TRS data from TRS-8-94	42

B-4. Sensor data, TRS-8-94 43
B-5. TRS data from TRS-9-94 44
B-6. Sensor data, TRS-9-94 45
B-7. TRS data from TRS-10-94 46
B-8. Sensor data, TRS-10-94 47
B-9. TRS data from TRS-11-94 48
B-10. Sensor data, TRS-11-94 49
C-1. Comparison of contour plot results, flux of TRS-8-94. 51
C-2. Comparison of topographical map, flux of TRS-8-94. 52
C-3. TRS-7-94. 52
C-4. TRS-8-94. 53
C-5. TRS-9-94. 53
C-6. TRS-10-94. 54
C-7. TRS-11-94. 54

LIST OF TABLES

Table		Page
1.	Effect of Temperature on Blackbody Emission	7
2.	Group Parameters	18
3.	Peak Values From Thermal Radiation Transmission Effect	26
4.	Peak Values From Thermal Conduction Effect	26
A-1.	TRS-3-92 Data	34
A-2.	Parabolic Fit Point Values	35
A-3.	Solutions for Parabolic Constants	36
A-4.	Location of Specified Fluence Along Map Points	36

Intentionally left blank

1. INTRODUCTION

In June 1993, during project MINOR UNCLE at White Sands Missile Range (WSMR), the Naval Surface Warfare Center (NSWC), White Oak Detachment, fielded an experiment with a composite material radome. Part of the testing was to evaluate the resistance of the composite to thermal radiation. The Defense Nuclear Agency (DNA), Field Command, provided an aluminum powder and liquid oxygen (LOX) Thermal Radiation Source (TRS) for the test. The radome was instrumented with thermocouples and strain gages on the inside and calorimeters on the opposite side of the TRS. The thermocouples were to measure the temperature vs. time profile of the inside surface during and after the deposition of radiant energy. The calorimeters were to ensure that the TRS replicated a previous thermal environment of interest. The data shown in Figure 1a are thermal radiation data measured during the test. The resulting radome thermocouple data, shown in Figure 1b, indicate a fast temperature rise and fall, followed by the expected exponential temperature rise due to heat conduction. Strain gages were also placed on the inside surface of the radome to measure deformation of the composite due to thermal effects. The strain gage data demonstrated a similar initial transient followed by the expected deformation attributed to heat conduction through the material. The initial transients were not consistent with theoretical calculations and needed to be explained.

After analysis by U.S. Army Research Laboratory (ARL) engineers, it was determined that the initial temperature and strain transients might be attributed to thermal radiation transmitting through the composite and directly heating the thermocouples and strain gages. The sensors were mounted on the panel backside and covered with a black tape. The tape was used to protect the sensors from environmental effects, such as dust, prior to the test.

It is thought that the black tape acted as a thin blackbody. Relative to the sensor, the large surface area of the tape absorbed nearly all of the transmitted thermal radiation. Since the backing was very thin, the total energy in the tape was quickly dissipated by conduction to the sensor and composite material and by natural convection on the exposed side of the tape. The degree of convection on the backside of the tape was small, and the composite acted as an adiabatic surface when compared to the highly conductive sensor material. As a result, the sensors were heated by the backing. When the TRS pulse ceased, excess heat in the tape dissipated quickly since there was very little heat capacitance, the temperature coming to equilibrium with the panel. As the panel backside started to increase in temperature, the thermocouple responded as predicted.

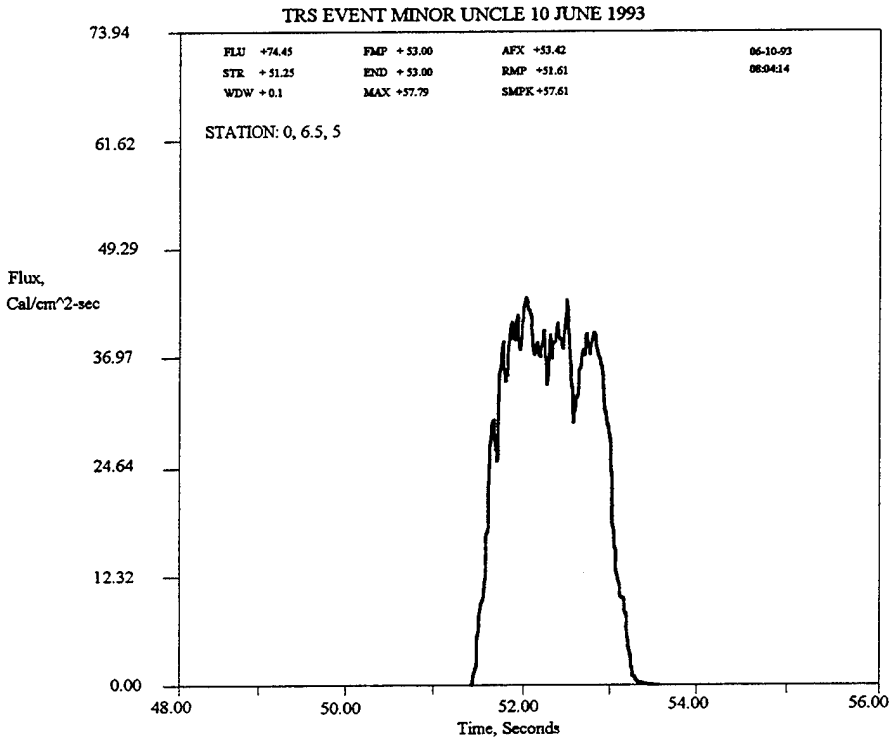

a) TRS Data.

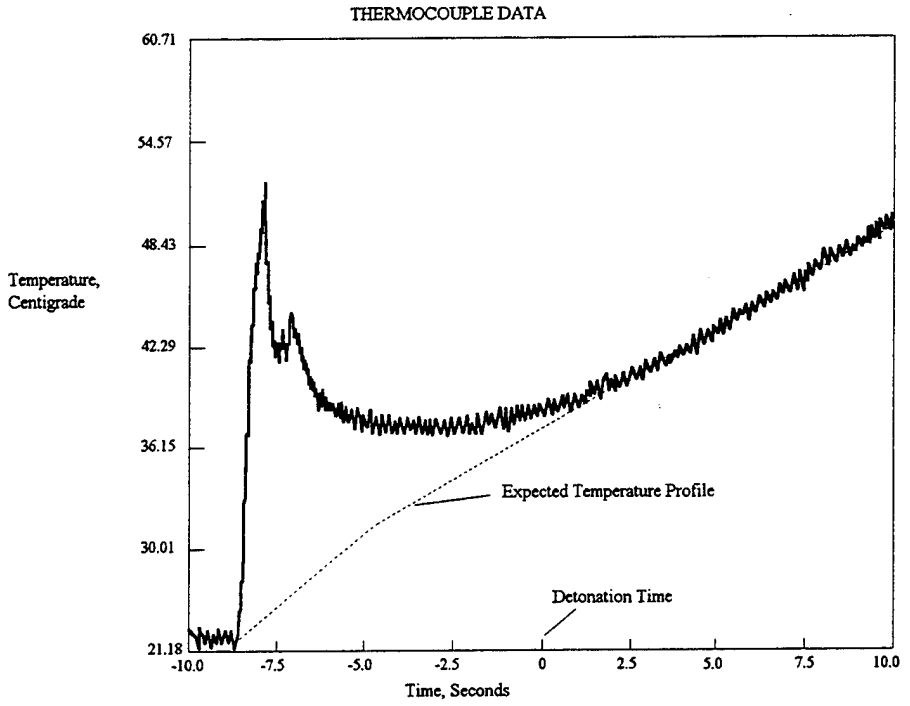

7

b) Thermocouple Data.

Figure 1. NSWC composite radome data.

In an effort to further investigate this hypothesis, NSWC and ARL conducted a series of experiments at the ARL TRS facility. The objectives of the experiments were to prove the theory about the tape backing affecting the temperature readings, to assess different methods of mounting thermocouples on thin composite panels for future testing, and to measure the amount of thermal radiation transmitted through the panel. Four rectangular composite panels were made with four thermocouples and two strain gages each, with various backings on each sensor. These panels were mounted on an aluminum box filled with insulation, creating an adiabatic surface on the backside of the panel. The aluminum box served to shield the sensors from direct thermal radiation, and to hold the panel in place during the experiments.

Each panel was used in separate TRS experiments. One panel was tested twice. The resulting data showed a repeat of the high transient thermal effects obtained during MINOR UNCLE, as expected. The data were analyzed to find any relationship between the TRS data and sensor data. The initial effects were compared between sensors to evaluate the effect of the type mounting/backing used. The amount of transmitted thermal radiation was measured. In evaluating the transmitted thermal radiation, the degree of protection afforded by the combustion of paint on the front surface of the panel was also determined.

2. COMPOSITE PANEL EXPERIMENT

The objective of the experiment was to prove that thermal radiation transmission through the composite radome accounted for temperature and strain transients in the initial part of the MINOR UNCLE data. It was desired to repeat the experiment. The TRS at ARL provided the same type of aluminum/oxygen TRS used by DNA. NSWC was able to obtain four composite panels of the same material and cover coating, with two different thicknesses. The panels were instrumented with the same type of sensors used at MINOR UNCLE. In addition, the ARL data acquisition system provided longer data recording on a digital system.

2.1 Thermal Radiation Simulator

The TRS at ARL uses aluminum powder combusting with LOX to produce thermal radiation on a target. The TRS is situated at Range 11 at the ARL Thermal Radiation Experimental Facility. The aluminum powder is blown by nitrogen from a storage vessel to the combustion chamber. Just prior to entry in to the combustion chamber, LOX is injected into the traveling powder. The mixture is ignited by pilot flames as it exits the nozzle. Momentum and combustion pressure causes the combustion mixture to rise several meters above the combustion chamber. The result is a large, highly luminous flame. The flame acts as a large blackbody panel with the hottest point radiating at about 3,000 K. Radiation from the flame is not uniform. It can be characterized by a specified **flux**, or rate of energy irradiating the target surface, and **fluence**, total irradiated energy on the target surface. Targets as large as 2 m^2 can be irradiated. Figure 2 shows the TRS as a free field source.

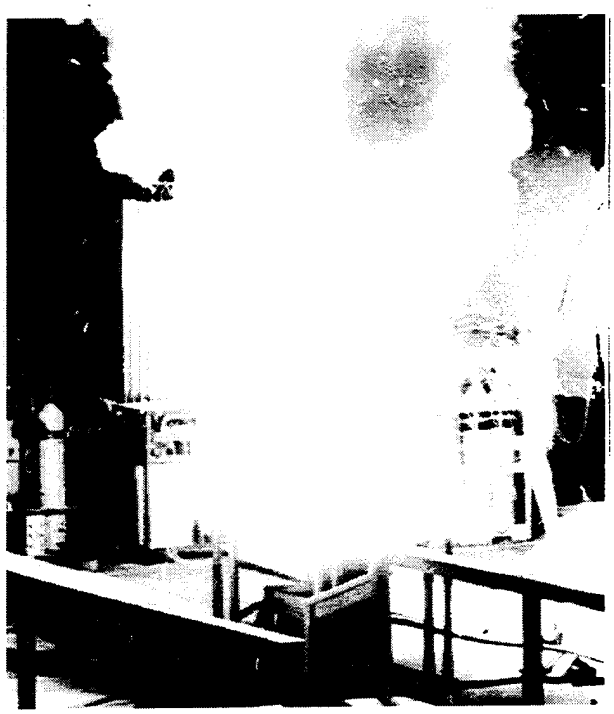

Figure 2. TRS unit as a free field source.

For the NSWC experiments, the primary nuclear weapon thermal parameter to be simulated was fluence. Flux was adjusted by placing the target nearer or farther from the flame. Since the TRS at ARL emits a rectangular shaped thermal pulse, as seen in Figure 3, the fluence was adjusted by setting the length of time of aluminum burn. The rectangular shaped pulse is excellent for controlling fluence.

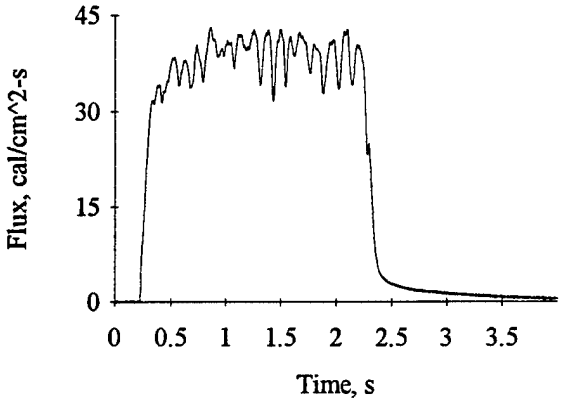

Figure 3. ARL TRS thermal simulation profile.

2.1.1 TRS Compared to Nuclear Weapon Thermal Radiation

The drawback of this type of simulator is the lack of fidelity with regard to a nuclear weapon when relating pulse shape, shape factor, and spectral color temperature. A true nuclear weapon thermal pulse is described by the dynamics affecting the resultant fireball. The nuclear weapon fireball emits about 40% of the total weapon energy in thermal radiation (Glasstone and Dolan 1977). Figure 4 shows a typical flux/time profile. As the fireball grows in size and rises above the ground, flux increases rapidly, and as the fireball expands beyond a certain radius, the radiant heat decays as the surface of the fireball cools.

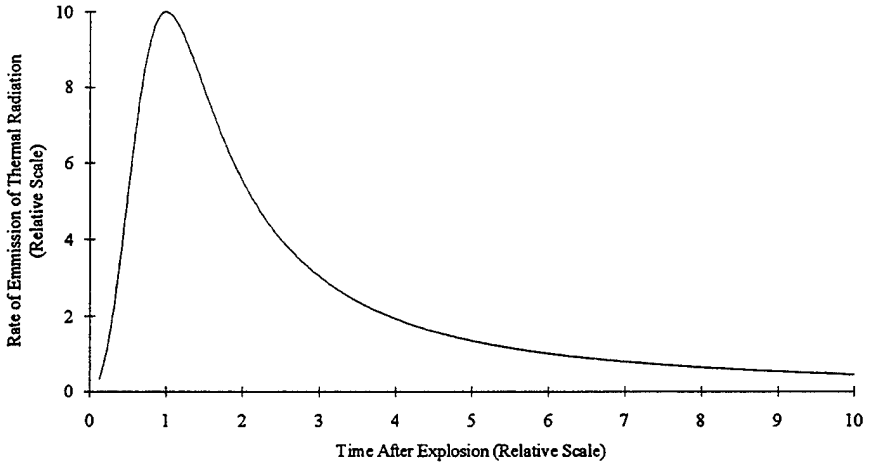

Figure 4. Nuclear thermal pulse profile, relative scale.

For a target that is expected to survive this type of environment, the pulse shape factor is fairly well determined as a radiant heat source that is very small and at a large distance from the target. The TRS is typically about 1 m from the target. During a TRS experiment, the back and sides of the target can have undesired exposure to thermal radiation. Care must be taken to prevent this in some experiments. The aluminum boxes used to mount the NSWC composite panels served to shield the back of the panels and attached sensors from direct thermal radiation.

The blackbody temperature of a typical nuclear fireball is about 6,000 K, which can be compared to the blackbody temperature of a TRS which is about 3,000 K. Almost 87% of the TRS radiant heat is in the infrared region (0.78 μm to 1,000 μm), the remainder in the visible light region (0.39 μm to 0.78 μm). A typical nuclear weapon has about 41% of its radiant energy in the infrared region, as much as 46% in the visible light region, and about 13% in the ultraviolet region (5×10^{-3} μm to 0.39 μm). Targets will be affected differently, but to what extent is difficult to surmise. This is quickly demonstrated by using the *Stefan-Boltzman law*:

$$E_b = \sigma T^4,$$

where σ is the Stefan-Botzman constant (5.670×10^{-8} W/m^2-K^4), and E_b is the emissive power of a blackbody at temperature T. *Planck's law* is given as

$$E_{b\lambda}(\lambda, T) = \frac{C_1}{\lambda^5\left(e^{c_2/\lambda T} - 1\right)},$$

where the constants values are generally accepted as

$$C_1 = 3.7413 \times 10^8 \text{ W-}\mu\text{m}^4/\text{m}^2,$$

and

$$C_2 = 1.4388 \times 10^4 \ \mu\text{m-K},$$

and the wavelength term, λ, is expressed in micrometers.

The blackbody emissive power shows a peak value. *Wien's law* can be deduced from Planck's and states that the maximum value of $E_{b\lambda}$ occurs at the wavelength given by

$$\lambda_{max} T = C_3,$$
$$= 2897.8 \mu\text{m} - \text{K}$$

The fraction of the total emission can be evaluated for specific values of wavelength. This is done by integrating the emissive power equation over the range of wavelength, which can be shown as

$$F_{0-\lambda}(T) = \frac{\int_0^{\lambda} E_{b\lambda}\, d\lambda}{\sigma T^4},$$

$$= \int_0^{\lambda T} \frac{C_1 d(\lambda T)}{\sigma(\lambda T)^5 \left(e^{C_2/\lambda T} - 1\right)}$$

The fraction of energy emitted between two wavelengths, λ_1 and λ_2, by a blackbody of temperature T is given as (Chapman 1984)

$$F_{\lambda_1-\lambda_2}(T) = F_{0-\lambda_2}(T) - F_{0-\lambda_1}(T)$$

Table 1 shows the effect of the different temperatures on the blackbody emission from the TRS at 3,000 K, and a nuclear weapon at 6,000 K.

Table 1. Effect of Temperature on Blackbody Emission.

Surface Temperature, K	3,000	6,000
Wavelength of maximum emission, μm	0.966	0.483
Total Emissive Power:		
W/m^2	4.59×10^6	73.48×10^6
cal/cm^2-s	108.9	1755.04
Spectral Fraction of Emission :		
Infrared (0.78 μm to 1000 μm)	0.8719	0.4092
Visible Light (0.39 μm to 0.78 μm)	0.1264	0.4626
Ultraviolet (5×10^{-3} μm to 0.39 μm)	0.0017	0.1212

Spectral color temperature effects on targets can be profound due to protection by coating or surface response. Objects shielded by the target (i.e., housings, covers) may transmit thermal energy differently. For instance, oil-based white paint will reflect up to 80% of visible light, but is essentially a blackbody absorber in the infrared. During a typical TRS experiment, a target coated with white oil-based paint would burn and char to a high degree. A total of 87% of the TRS energy in the infrared would be absorbed by the target. Of the remainder in the visible light, 70% would be absorbed. About 91% of the total thermal radiant energy would be absorbed by the target. In the nuclear environment with the same thermal radiation load, the same target would be

significantly less damaged. The white paint would reflect about 37% of the visible light and absorb the remaining 41% of the infrared, thus loading the target with only 78% of the thermal radiant energy. Transmissive material properties are also subject to the same effects.

2.1.2 TRS Simulation Profile

The TRS at ARL is the product of several years of improvement to enhance the flux and fluence repeatability between experiments (Loucks, Muller, and Thane 1994). It has served as a prototype for integration with the ARL 2.44-m probative shock tube and as a test-bed for state-of-the-art TRS performance improvements. When a TRS is incorporated into the 2.44-m tube, it will provide an excellent test-bed facility for simulated nuclear thermal and blast synergistic loading experiments. However, it has been determined that, despite improved simulation performance, the TRS is incompatible with the desired integration. The TRS continues, however, to serve as an excellent simulator for experiments requiring high radiant heat for about 500 ms. At the present time, the TRS remains in the 2.44-m tube section as depicted in Figure 5.

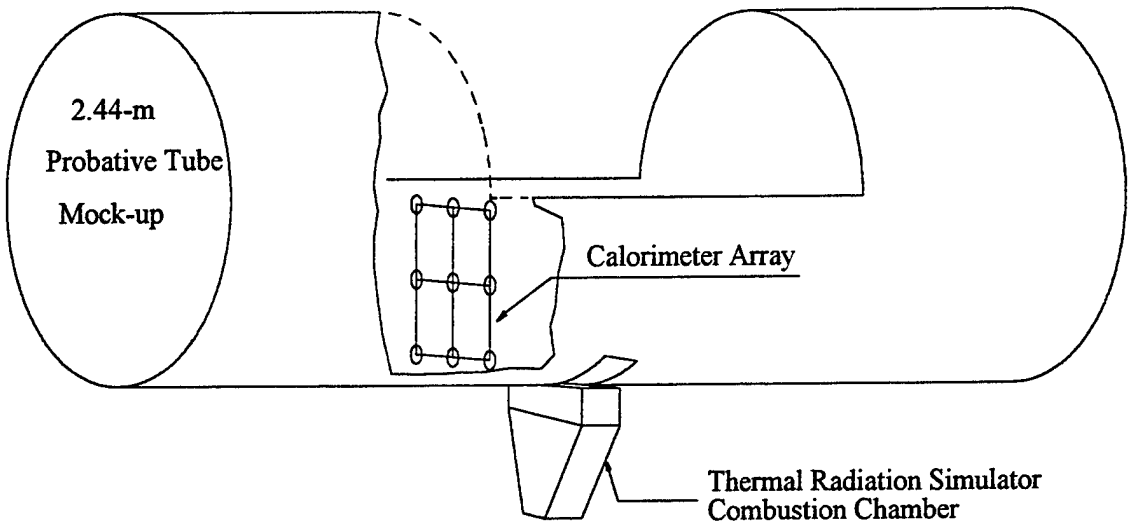

Figure 5. 2.44-m probative tube and TRS showing calorimeter array.

Data collected for several years from the ARL TRS have resulted in a thermal database. Figure 6 shows a typical contour plot of isoradiance on a plane 100 cm away from the center of the TRS (Loucks 1991). Each contour line represents fluence for a given experiment. Data between various calorimeters used during experiments were interpolated with a second-order curve fit and, in the same manner, extrapolated to the area outside the calorimeter region. A smooth curve was used to connect the resultant decade flux levels. For a more detailed explanation of this process, see Appendix A.

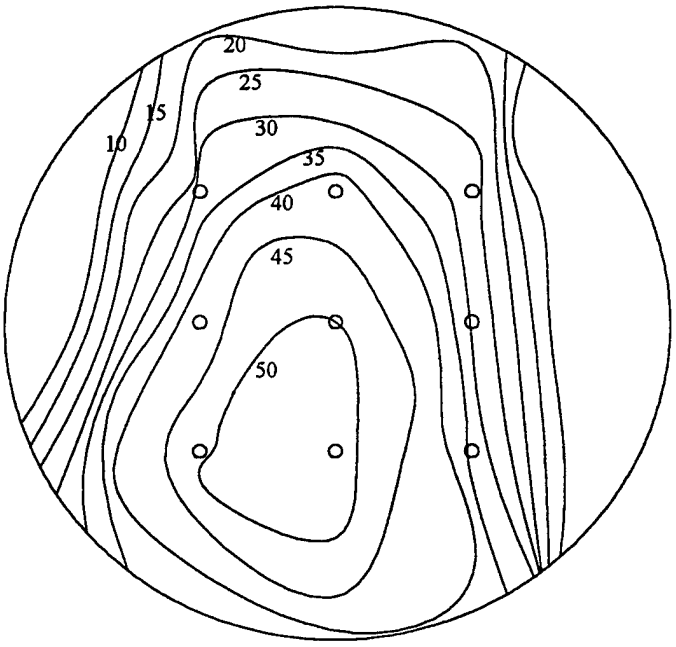

Figure 6. Contour plot of isoradiance at 100 cm from center.

It is evident from the contour plot that thermal irradiance from the TRS is not symmetric about the vertical axis. This peculiarity persists, even in different wind conditions. A theory of why this occurs is related to the method in which the aluminum powder is transported to the combustion chamber. The aluminum powder is stored in a pressurized vessel about 15 m from the combustion chamber. A 5-cm-diameter copper tube spans the distance. The aluminum powder is transported through the pipe by means of nitrogen gas blowing through the pipe. Just before it reaches the combustion chamber, the aluminum must turn 90° in a special copper tube. The tube is constructed such that the cross section is circular during the turn. The turn is a gradual curve, as opposed to an elbow fitting, with a radius of curvature at about 75 cm. This was done to minimize flow restriction. The 90° bend may be the cause of the asymmetry in the thermal map. Aluminum powder may concentrate on one side of the tube running in the vertical

direction. When the LOX is injected into the powder, the rotational momentum must turn the concentration to the opposite side. When the mixture enters the combustion chamber, a higher concentration may be on one side, resulting in the asymmetric thermal mapping. This is not particularly detrimental to TRS performance, but it does limit the size target that can be tested with uniform irradiance. Asymmetrical irradiance also limits application of the TRS to the probative shock tube. Target placement is normally in the center of the tube cross section. Due to the asymmetry, the maximum radiation would be shifted to one side of the tube.

For small targets, approximately 30 cm by 30 cm, this is not a problem, and the ARL TRS performs well. NSWC personnel wanted to repeat the MINOR UNCLE experiment, but with small flat panels as opposed to a full-scale radome. This was primarily due to cost constraints, flat panel specimens being much less expensive to test than a full-scale radome. The procedure for the NSWC experiments at ARL would be simple; perform about three TRS experiments to locate the area of desired flux and fluence, then test each panel individually. The desired loading levels were **50 cal/cm^2-s** flux and **75 cal/cm^2** fluence. The pretest firings were done with 10 calorimeters, 9 of which were spaced 45 cm apart in an even rectangular array in 3 rows of 3 calorimeters. The remaining calorimeter was placed on the opposite side of the TRS to help evaluate consistency of the TRS with prior experiments. The results of these experiments resulted in contour plots of an average flux and fluence presented in Figure 7.

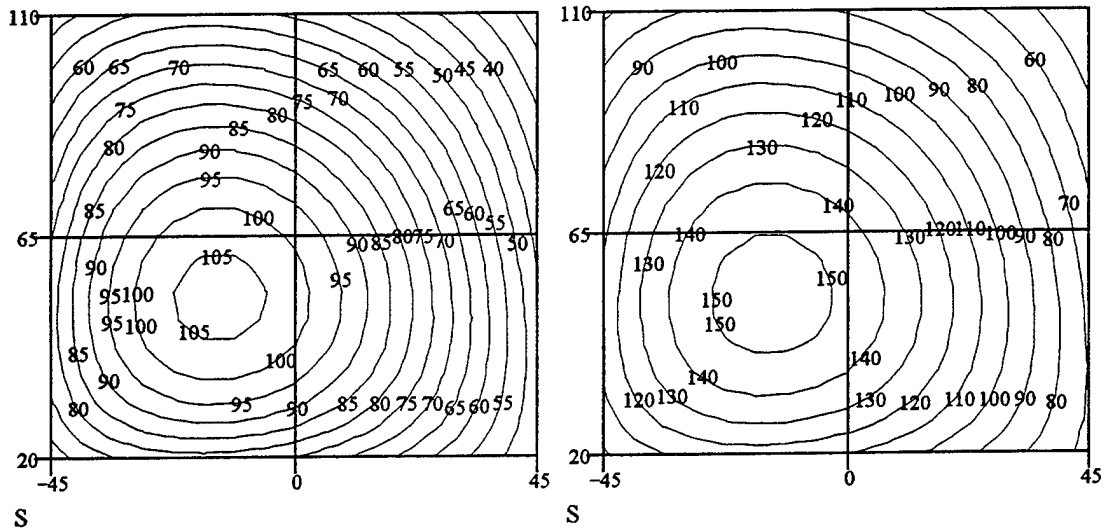

Flux, cal/cm^2-s Fluence, cal/cm^2

Figure 7. Pre-experiment contour plots at 60 cm.

Unlike the parabolically smoothed contour lines shown in Figure 6, the isoradiance contours seen in Figure 7 are linearly derived from the fluence data of the nine calorimeters during a given test. The desired thermal loading was determined to be in the middle of the upper right hand quadrant. This was selected because of ease of mounting the target to the calorimeter frame. The average flux is derived using a Fourier Averaging Method (Loucks 1990).

2.2 Experiment Setup

The NSWC tested a fullscale radome during the MINOR UNCLE experiment. To investigate the effect of infrared (IR) transmission, NSWC used four rectangular panels made of the same material as the radome. This was done to reduce the cost of the IR experiment since the material would be destroyed with each experiment. The panels were readily available. A radome would have taken a great deal of time to fabricate and deliver. Another advantage of using the panels was that extra panels could be tested to verify reproducibility of the TRS and experimental procedure. Several methods of mounting the thermal and strain sensors could be tried and evaluated, and the thermal loading could be varied for each experiment.

Each test panel was made from a fiberglass/epoxy composite. The panels were of two different thicknesses, 3.17 mm and 6.35 mm. Each panel was 20.32 cm by 30.48 cm in size except the last panel. It measured 6.35 mm in thickness and was 30.48 mm by 30.48 mm. All panels were coated with a glossy white polyurethane paint. The edges and back were bare. The thermocouples and strain gages were mounted on the back, as shown in Figure 8.

2.2.1 Instrumentation

The TRS facility at ARL is set up primarily to perform research concerning the simulation of nuclear thermal radiation. Much of the thermal radiation simulator assessment is done by direct measurement of the TRS output and its effect on experimental targets. The data acquisition system at the ARL TRS facility is a MEGADAC 2200C, manufactured by OPTIM Electronics. A personal computer (PC) controls the TRS and the MEGADAC. The MEGADAC operates sequentially, sampling data from each channel in a stacked fashion. The data are stored digitally in the MEGADAC and retrieved with the PC when desired. Figure 9 shows the schematic setup of the controller and data acquisition system and the way the components are linked together through the PC (Loucks, Muller, and Thane 1994).

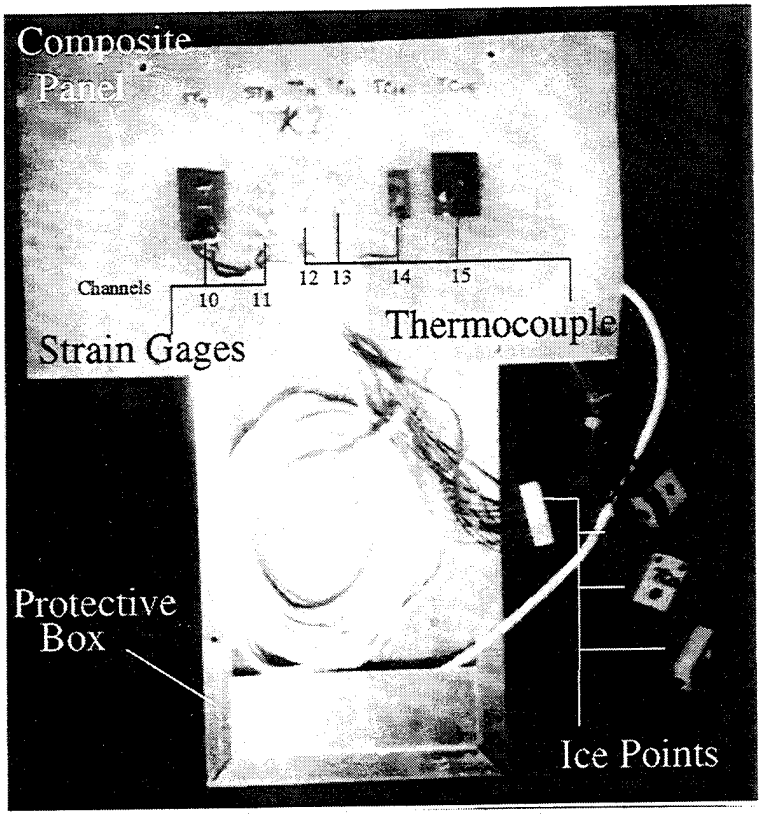

Figure 8. Composite panel with sensors mounted on back.

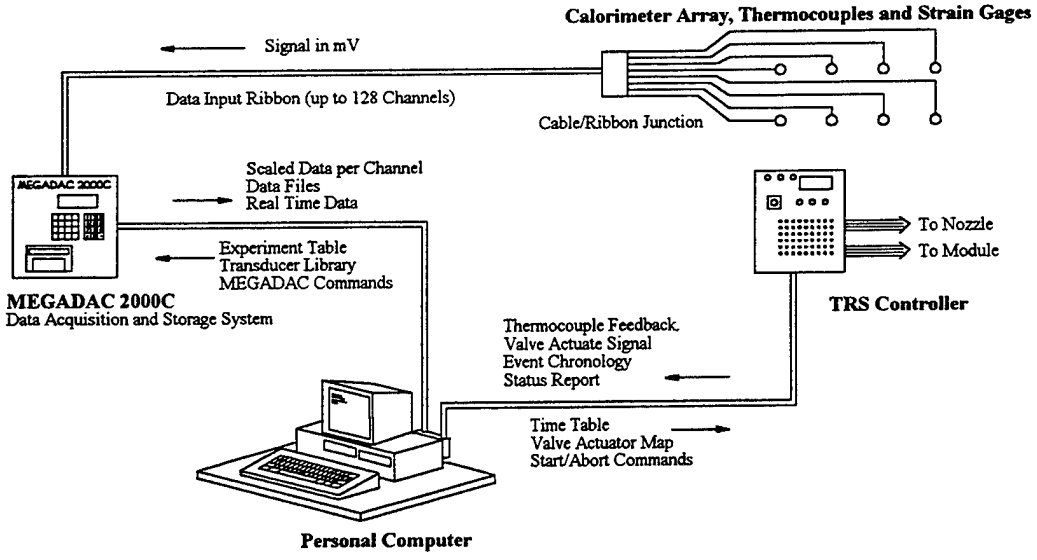

Figure 9. Controller and MEGADAC.

The Gardon-type gage is the primary transducer used to measure thermal flux. As shown in Figure 10, the gage is basically a constantan diaphragm welded to a copper wire and body. This particular construction generates two thermocouple junctions. The diaphragm acts as the heat transfer sensor while the main copper body acts as a heat sink.

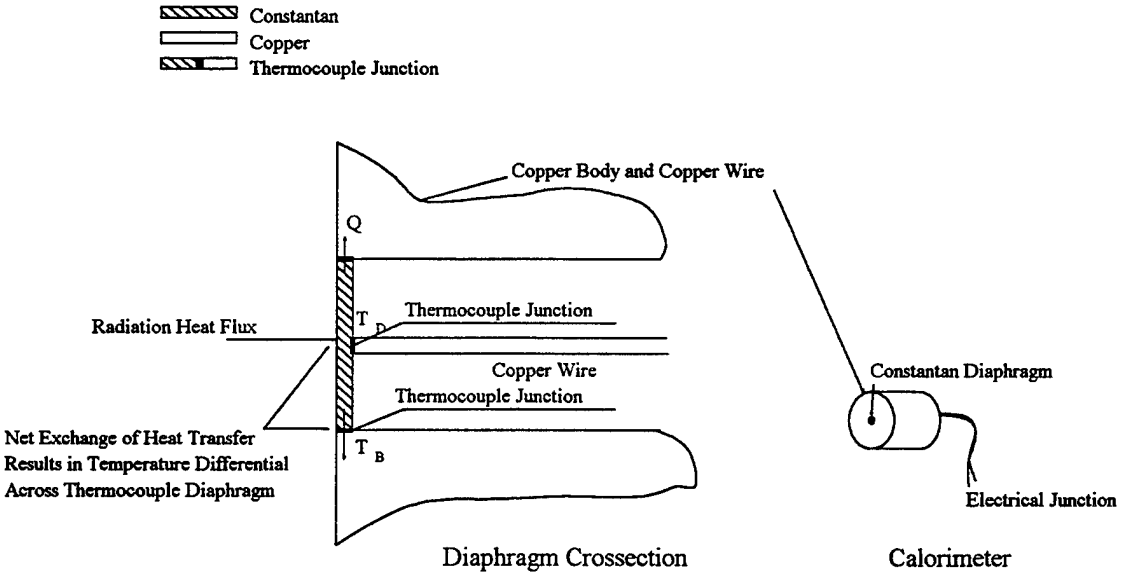

Figure 10. Gardon-type gage for flux measurement.

The Gardon-type calorimeter produces a measurable voltage when a temperature difference is produced between the two thermocouple junctions. This voltage can be represented as

$$V_m = C_{TC}(T_D - T_B),$$

where

V_m is the voltage produced from calorimeter,

C_{TC} is a proportionality constant,

T_D is the diaphragm center temperature, and

T_B is the diaphragm edge temperature.

2.2.2 Experiment Setup and Process

During the NSWC test, the TRS, instrumentation array, and composite panels were set in a mocked-up section of the 2.44-m probative tube, which was depicted earlier in Figure 5. The photograph in Figure 11 is an NSWC composite panel mounted on the test frame. The custom-made frame was fabricated for a similar, previous test of a larger panel.

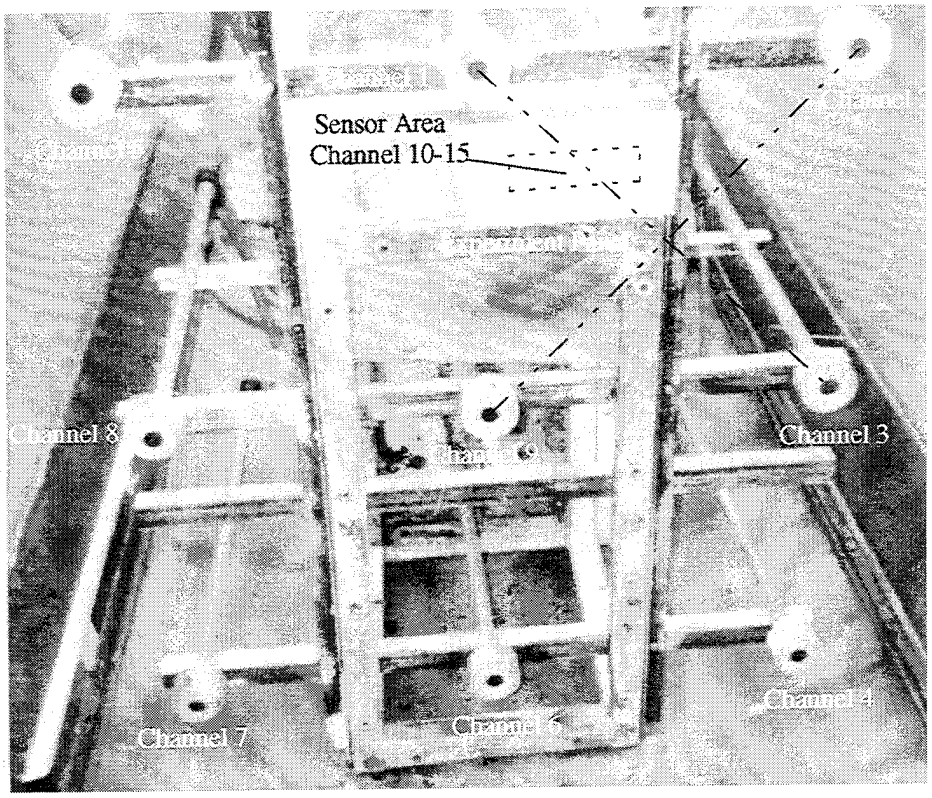

Figure 11. Composite panel on calorimeter array frame.

All NSWC composite panels were mounted in the upper right quadrant of the calorimeter array. This location was chosen after reviewing the data shown in Figure 7. Instrumentation cables were run out the end of the 2.44-m tube through a metal flexible conduit. The conduit was used specifically to protect the cables from thermal effects. All junctions were connected in a junction box with terminal strips. Cables from the junction box traveled underground in a PVC conduit to the instrumentation control bunker. In the bunker, the cables were terminated on junction cards made specifically for the MEGADAC 2200C.

Output voltages from all calorimeters and thermocouples were connected directly into the MEGADAC 2200C as described. Strain gages passed from the junction box to a portable two channel Wheatstone bridge network located in the bunker. Output from the bridge network was connected to the MEGADAC through the junction cards.

Transducers were examined and tested for continuity and channel assignment before each test. Calorimeters were visually examined and tested by briefly applying a flame from a hand-held propane torch to the calorimeter in question and observing the response on the computer screen. The thermocouples and strain gages were visually checked for secure mounting and condition, and were electrically examined for continuity, but they were not tested for functionality as were the calorimeters.

The TRS was operated at least once before each experiment to ensure the system was functioning properly. Once the TRS was determined to be performing as expected, and the instrumentation was verified as operating as expected, the experiment proceeded. The panel was secured to the mount, the instrumentation was monitored, and the experiment countdown was initiated.

Each component of the TRS system requires a finite amount of time to function. An example is preflowing of LOX to the nozzle to precool and condition the LOX delivery system. This is done to ensure that there is adequate oxygen for stoichiometric combustion. The line that supplies the LOX is cooled for about 10 s by flowing LOX while diverting the LOX away prior to the mixing point in the nozzle. As the LOX pipe cools, the LOX evaporation rate inside the line is decreased. The result is that nearly all of the oxygen that enters the mixing chamber is in liquid form. This supplies enough oxygen mass flow to provide stoichiometric combustion with the aluminum powder. The aluminum powder must also be preflowed to establish a steady mass flow rate to the nozzle. The stoichiometric mixture flows past the pilot flames, ignites, and produces high-intensity thermal radiation on the target panel, as can be seen in the photograph in Figure 12.

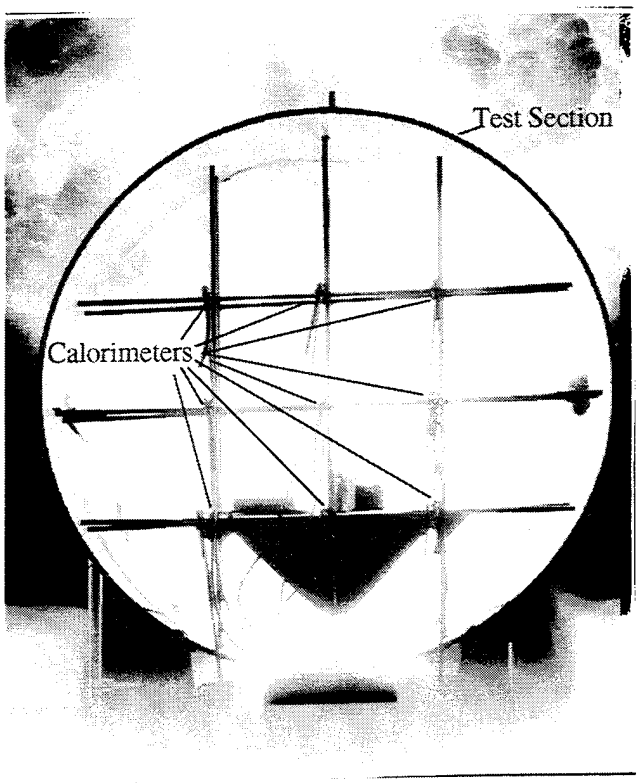

Figure 12. TRS in test section.

2.3 Post Experiment Process

After each experiment, collected data were transferred from the MEGADAC to a personal computer via an IEEE interface. An ASCII file was created for each data channel and saved on two hard drives and a floppy disk. The beginning of each file had a header section that contained information about that particular channel in the following format: experiment title, experiment number, transducer station, abscissa label, abscissa units, ordinate label, ordinate units, time of arrival and time between samples, in milliseconds, and the number of data points. The data point values immediately followed. This was done so that the data were easily transported to another system for analysis by other researchers.

A quick look at the data immediately revealed that the effect experienced at WSMR was being repeated. The sensors were generating a highly transient signal before the thermal conductive effects could be applied.

3. DATA ANALYSIS

There were five TRS experiments. The last panel was tested twice. The data were successfully captured by the MEGADAC 2200C and transferred for analysis on a personal computer. A software product called DADiSP 3.0 was used to analyze the data. DADiSP was limited in only being able to create Fast Fourier Transforms of the data sets. Full Fourier Transforms of the data were performed with a utility written for that purpose (Loucks 1988). Extraction of the forcing mechanism was used to verify that the TRS energy was directly affecting the sensors on the panel backside. All the data acquired from these experiments are plotted in Appendix B.

Both the thermocouple and strain gage data repeated the initial high transient phenomenon found in the MINOR UNCLE data. The initial temperature increase is theorized as being a result of the thermal radiation from the TRS directly irradiating the sensor and the material used to mount the sensor. Typically, metals have a very low thermal radiation absorptivity coefficient, α'_n, across all ranges of thermal radiation (typically $\alpha'_n = 0.18$ for a highly polished surface, and $\alpha'_n = 0.75$ for a heavily oxidized surface). The thermocouples used in these experiments were highly polished due to the thermocouple junction being joined by soldering and the solder cooling with a smooth, highly reflective surface,resulting in $\alpha'_n \approx 0.07$. The strain gages were observed to also have a highly polished surface. This indicates that the majority of the radiation incident to the sensor would be reflected back into the composite material. This thermal energy would eventually be conducted back to the sensor. Any material used to mount the sensor is obviously in contact with a large portion of the sensor surface. The thermal radiation incident to a large absorptive foil, such as black vinyl tape, used to secure a sensor to the panel may have absorptive coefficients ranging from $\alpha'_n = 0.20$ for aluminum tape to $\alpha'_n = 0.88$ for black tape. The relatively large area of the backing would act as a thermal collector, and the heat would conduct to the sensor and the area of composite in contact with the backing. In general, the area thermal state would increase in proportion to the amount of thermal energy irradiating in the components.

In order to prove this, sensor data would have to be directly related to TRS data. Two techniques were explored. The Fourier Transforms of the TRS data and the sensor data were compared for common frequencies. An additional technique actually used sensor data to reveal the TRS data by filtering out the expected material response and isolating the transient effects. A method of extracting the influencing function was compared to the TRS data to see if the forcing function matched the influencing function.

3.1 TRS Data

All TRS data were captured. An unexpected flare of flames from the panel on the last experiment caused the level of one channel, channel 1, to go so high that the output voltage exceeded the upper band-edge of the recording device, thus the true peak level of the data for that channel on the last test is unknown. Recorder sample rate was 200 Hz. Flux levels were expected to range from 30 cal/cm^2-s to 120 cal/cm^2-s for brief periods. Desired fluence levels for the experiment dictated the TRS burn for 1.5 s. Figure 13 shows the data captured from channel 9, the low center calorimeter, for all five experiments. TRS titles correspond to the experiment. TRS-7-94 was the first experiment, TRS-8-94 was the second, etc. Table 2 lists important parameters from each experiment. Appendix C shows the flux and fluence contour maps for each experiment.

Table 2. Group Parameters

TRS Station	TRS-7-94		TRS-8-94		TRS-9-94	
	Flux	Fluence	Flux	Fluence	Flux	Fluence
-60/-45/110	42.49	46.39	34.55	47.64	44.44	46.60
-60/0/110	46.56	51.16	34.64	48.37	49.28	53.09
-60/45/110	21.76	25.77	17.00	24.99	29.41	29.35
-60/-45/65	68.83	75.04	63.48	87.74	73.91	76.97
-60/0/65	88.97	101.12	83.50	116.27	99.22	105.81
-60/45/65	35.33	39.73	30.73	43.49	43.31	42.11
-60/-45/20	68.41	72.63	66.96	93.08	69.98	73.77
-60/0/20	72.46	79.87	73.78	103.94	76.39	81.59
-60/45/20	43.26	49.16	41.56	58.00	39.72	43.78

TRS Station	TRS-10-94		TRS-11-94	
	Flux	Fluence	Flux	Fluence
-60/-45/110	35.46	15.31	40.67	143.029
-60/0/110	52.00	20.63	60.00	222.00
-60/45/110	23.90	9.43	21.41	80.41
-60/-45/65	48.42	19.67	70.726	250.47
-60/0/65	84.86	33.05	89.45	334.16
-60/45/65	30.37	12.44	41.73	151.92
-60/-45/20	48.92	18.66	64.74	234.84
-60/0/20	66.72	25.23	74.47	273.34
-60/45/20	27.64	11.46	44.32	164.57

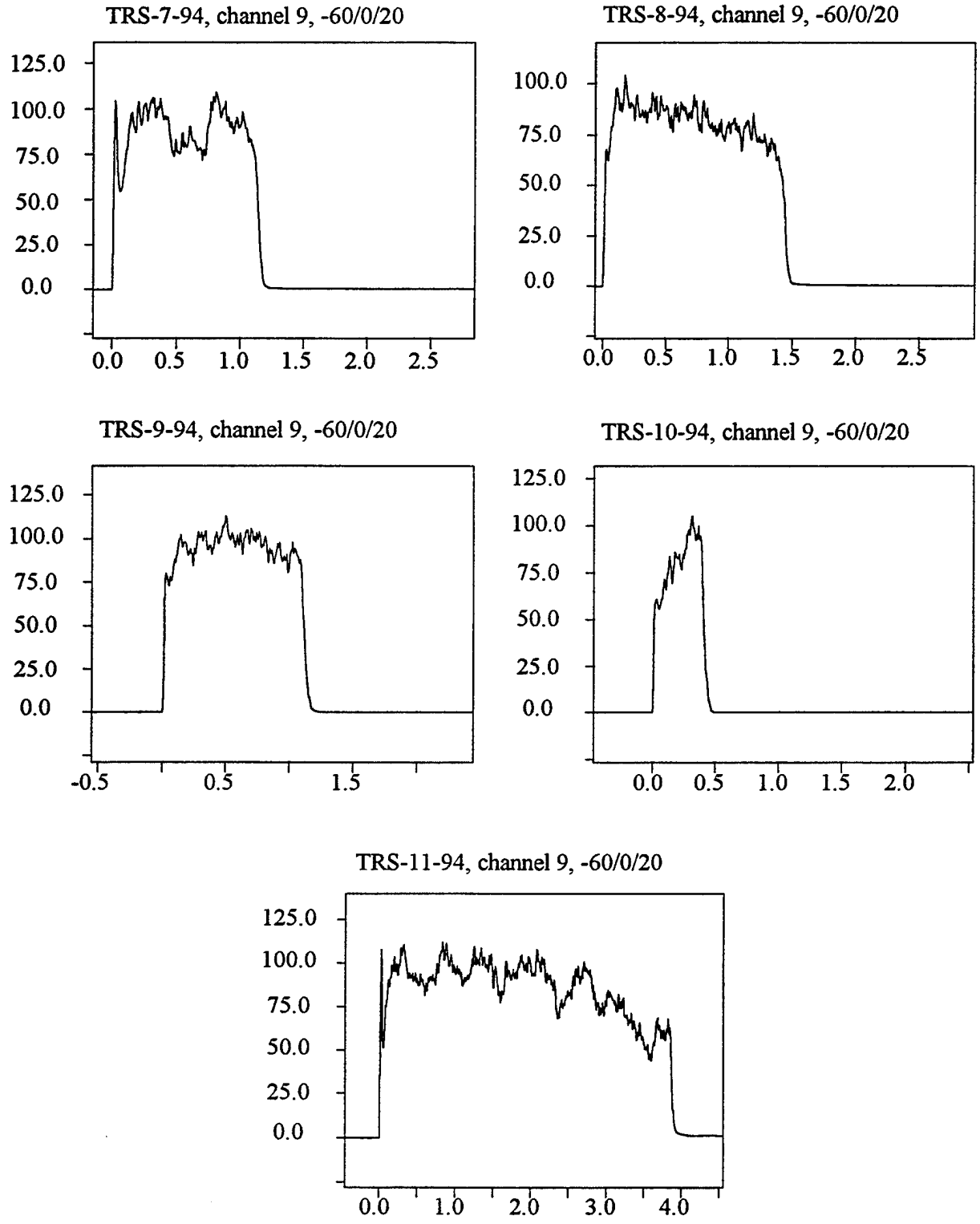

Figure 13. Thermal radiation data for each experiment at channel 9.

3.2 Thermocouple and Strain Gage Data

Thermocouple and strain gage data were collected during each test for a period of 60 s. This time interval permitted collection of early transients as well as the longer term response. In all cases, the thermocouple data were good. The strain gages were more delicate, and some channels of strain data were lost during the experiments. The data were captured using the same data acquisition system as the TRS data. The sample rate was 200 Hz. The thermocouples were connected to commercial ice points, then the signal sent directly into the MEGADAC. The strain gages were conditioned through a two-channel Wheatstone bridge/amplifier, and the resultant signal sent to the MEGADAC.

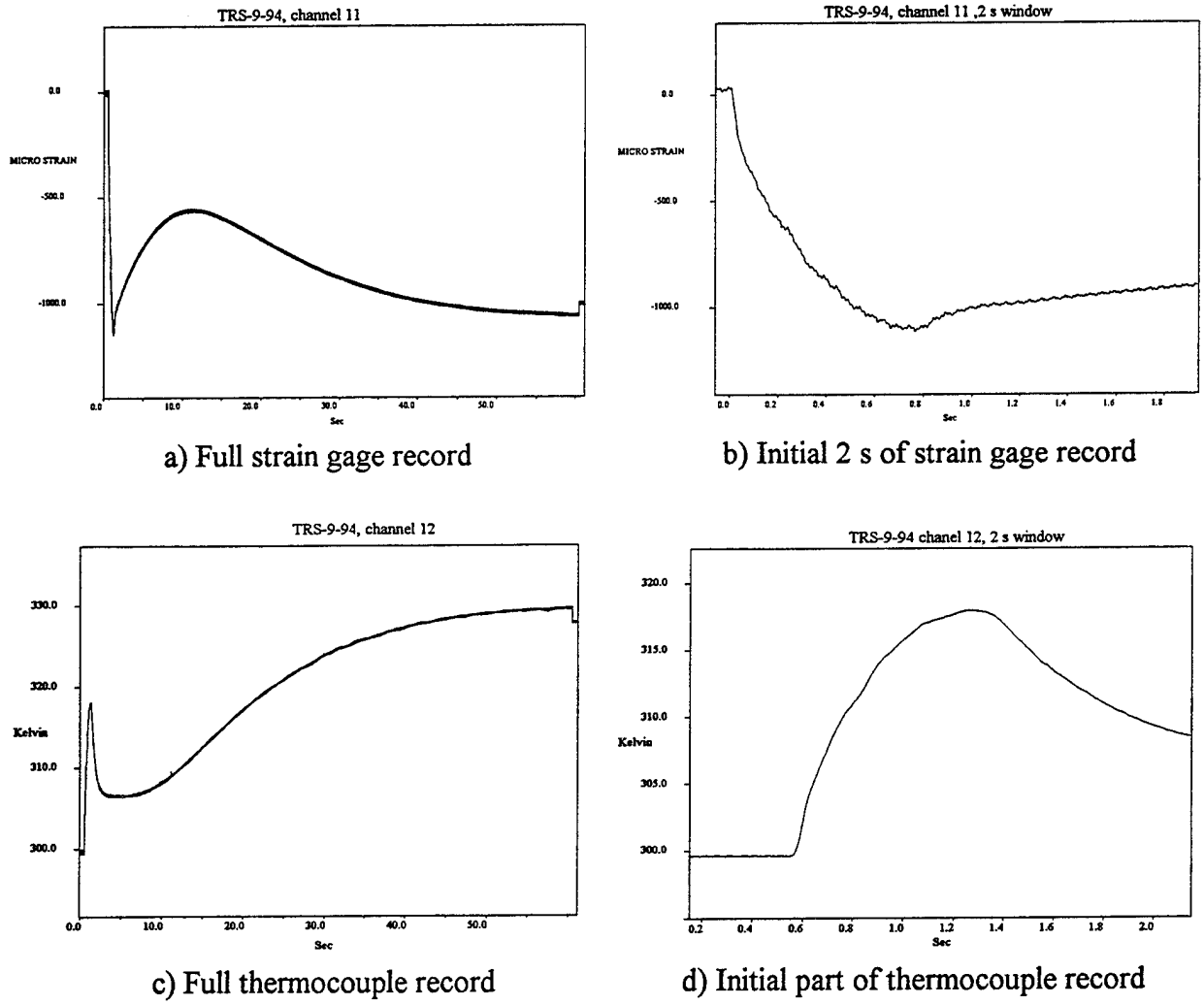

a) Full strain gage record

b) Initial 2 s of strain gage record

c) Full thermocouple record

d) Initial part of thermocouple record

Figure 15. Sensor data from channel 12 and 13, TRS-7-94.

Data from the thermocouples exhibited the same transient phenomenon found in the data from the MINOR UNCLE test. Figure 15 shows the channel 12 thermocouple from TRS-10-94, the only experiment with a complete data set. The distinct initial transient is evident. Figure 16 shows the calorimeter data from the closest calorimeter to the panel.

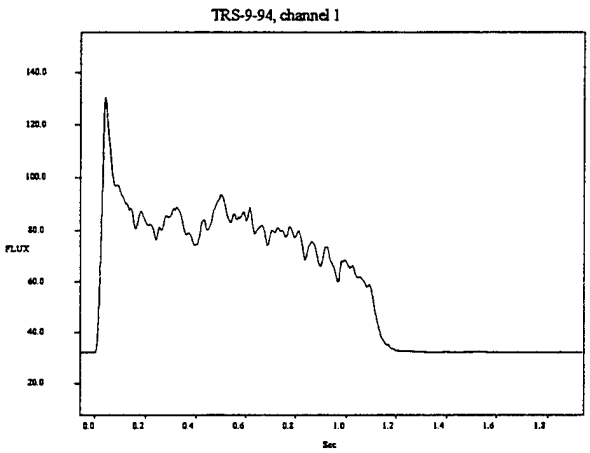

Figure 16. TRS-9-94, calorimeter closest to composite panel.

3.2.1 Fourier Transform Analysis.

To identify the source of the transient, it was suggested that a Fourier Transform of the data out to 20 Hz might show a relation between the TRS data and the thermocouple data. A numerical program (Loucks 1988) was used to take the direct Fourier Transform of the data. The results of that transform is shown in Figure 17. The Fourier Transform being defined as

$$G(f) = \int_{-\infty}^{\infty} F(t)e^{-i2\pi f}dt,$$

where

f is frequency,
t is time,
$G(f)$ is the transformed function in the frequency domain, and
$F(t)$ is the function in the time domain.

The Fourier transform can be used to identify features in the frequency domain that are masked in the temporal domain. The result of such a transformation results in real values and imaginary values. The magnitude of the Fourier transform is the square root of the sum of the squares of the imaginary and real components. The transform was not taken out any further than 20 Hz. The magnitude of the signal beyond this frequency is well within the noise band of the instrumentation.

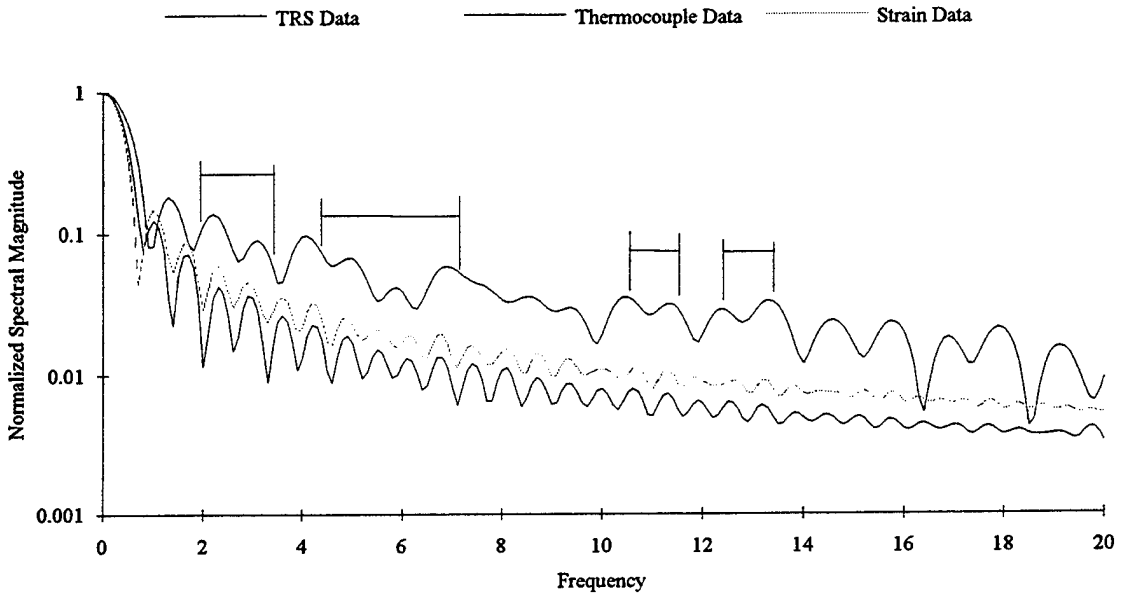

Figure 17. Magnitude of Fourier transform of thermocouple data and TRS data.

Few relational features between the TRS data and the sensor data are outstanding in the Fourier Transforms. There is a strong comparison at intervals in the record. These are pointed out by the brackets in Figure 17. If one were to express the transforms in terms of the coefficients of a Fourier series, the thermocouple and strain gage data coefficients would match very well. One could conclude that the phenomenon influencing the thermocouple is the same phenomenon influencing the strain gage. The TRS data coefficients are different. There are points of similarity, such as at 3, 6, 11, and 13 Hz. This indicates the influence of thermal radiation transmission from the TRS. The relation between the sensor response and the transmitted thermal energy is circumstantial, and far from conclusive.

3.2.2 Forcing Influence Extraction From the Data

A method of extracting the forcing influence from the response data was derived to demonstrate direct thermal radiation energy influence on the gages. The method involved several steps which are outlined in this section. An example is shown using thermocouple data described in the previous section.

The first step was to determine the signal that was likely to occur without any initial transients. This can be done in one of two ways. The first way, which is much more difficult, would be actually to calculate the target response without transmission effects. An analytical method and a numerical simulation using finite differencing (Loucks 1990) are two possible ways to obtain the response. The second and easier method was to make a simple curve fit of the data without the initial transient. By eliminating a short period of the initial data, a least-squares fit of the slower response was made. Figure 18 graphically illustrates a fifth-order polynomial least-squares fit of the thermocouple data with the first 12.5 s of data removed.

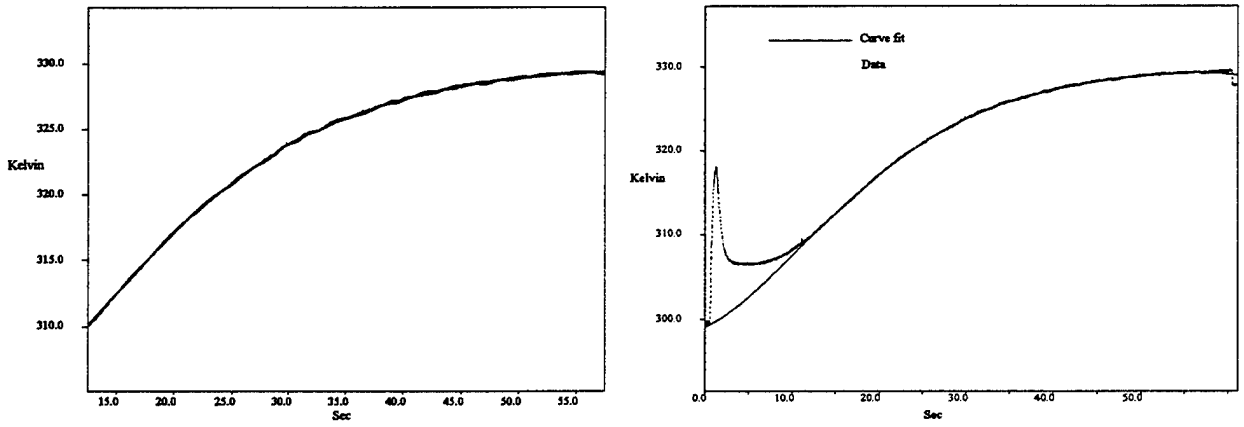

a) Slow response portion of data.

b) Polynomial curve fit with data

Figure 18. Obtaining a curve from data.

The polynomial used in this curve fit was

$$T(t) = 298.4926 + 0.82904t + 0.10505t^2 - 4.5249 \times 10^{-3} t^3 - 6.976 \times 10^{-5} t^4 - 3.9 \times 10^{-7} t^5,$$

where $T(t)$ is the temperature in degrees Kelvin, and t is time in seconds.

The second step was to subtract the curve fit from the data to isolate the initial transient. Figure 19 demonstrates this step.

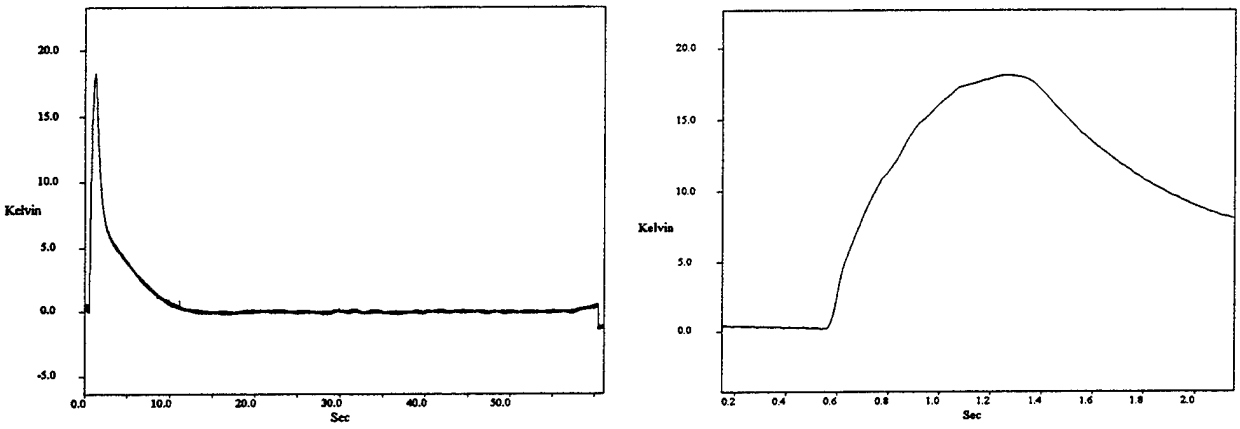

a) Full difference curve

b) Initial portion of difference curve

Figure 19. Initial transient isolated from conduction data set.

The curve in Figure 19b appears exponential in form. A thermocouple has an associated, first-order response time. One could conclude that the influencing phenomenon which caused the thermocouple to gain heat is masked by thermocouple response time. If the thermocouple acted as an ideal transducer, the curve of Figure 19 would appear quite different. In fact, it would show the influence in great detail. Using a method to compensate transducer output to that of an ideal, rapid rise time transducer (Loucks, Muller, and Thane 1994), the influencing phenomenon is revealed in Figure 20. The method is to take the signal and add to it its first derivative multiplied by a constant,

$$\mathrm{T}i = \mathrm{T}m + \frac{1}{C_t}\frac{d\mathrm{T}m}{dt},$$

where Ti is the actual temperature if the influencing phenomenon, Tm is the thermocouple output, C_t is the rise time constant, and t is time.

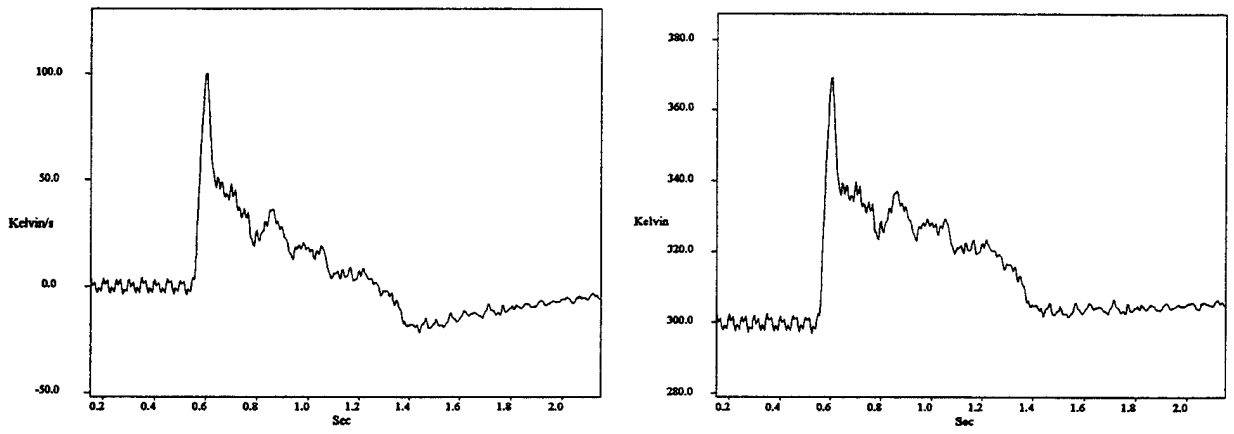

a) Derivative of isolated signal

b) Compensated signal

Figure 21. Compensated transducer signal.

The final step was to compare the compensated signal with the nearby calorimeter signal. If the signals are similar, then the TRS output can be directly linked to the initial transient signal. Figure 22 compares the TRS output that was shown in Figure 16 and the compensated signal results from Figure 21b. The traces have been normalized (divided by the maximum positive value in the data set) for comparison.

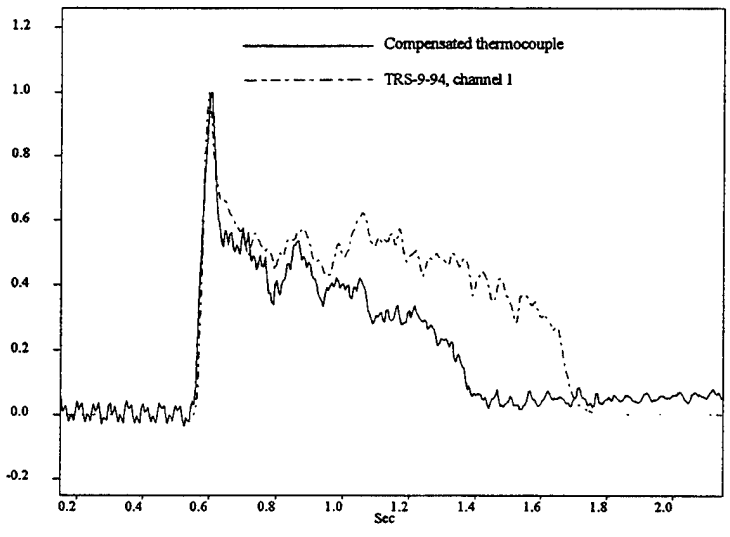

Figure 22. Comparison of normalized signal.

This result demonstrates a clear relation between the initial influence and the TRS output. The signals are identical in the initial 0.1 s. Eventually the thermocouple signal diverges away from the TRS signal with time. This can be attributed to the composite material or the coating on the front face undergoing a property change. At about 0.8 s into the event, the transient thermocouple signal dropped, even though the TRS was still burning. It was later discovered that this was when the painted surface started to emit smoke, protecting the composite material from further direct thermal radiation damage.

4. RESULTS

4.1 Thermal Effects Due to Different Mounting Methods

The different mounting used to secure the sensors to the rear face of the panel resulted in a difference in how each sensor responded. The heating effect by thermal radiation transmission is increased when using a backing that is a good thermal radiation absorber. The bare sensors reached a higher peak value when a backing was used. The higher the absorptivity of the backing, the higher the peak value measured. Figure 23 demonstrates this from TRS-10-94. Table 3 lists the temperature and strain values reached for each experiment.

Table 3. Peak Values From Thermal Radiation Transmission Effect

Channel	TRS-7-94	TRS-8-94	TRS-9-94	TRS-10-94	TRS-11-94
10: Bare Strain Gage	NA	-1703 με	NA	-5139 με	-6446 με
11: Black Backed Strain Gage	NA	-726.9 με	-1137 με	-2862 με	-4011 με
12: Bare Thermocouple	384.6 K	NA	317.8 K	356.2 K	379.1 K
13: Bare Thermocouple	383.2 K	NA	314.6 K	352.6 K	375.8 K
14: Acrylic Backed Thermocouple	406.8 K	324.7 K	314.1 K	370.3 K	402.7 K
15: Black Backed Thermocouple	395.4 K	NA	321.4 K	400.2 K	455.7 K

Table 4. Peak Values From Thermal Conduction Effect

Channel	TRS-7-94	TRS-8-94	TRS-9-94	TRS-10-94	TRS-11-94
10: Bare Strain Gage	NA	-1250 με	NA	-1965 με	–5318 με
11: Black Backed Strain Gage	NA	-969.9 με	-1059 με	-1453 με	–5126 με
12: Bare Thermocouple	399 K	NA	329.4 K	344.5 K	466.94 K
13: Bare Thermocouple	399.6 K	NA	330.1 K	342.6 K	464.7 K
14: Acrylic Backed Thermocouple	406.2 K	NA	330.3 K	341.6 K	NA
15: Black Backed Thermocouple	414.7 K	NA	330.5 K	344.2 K	NA

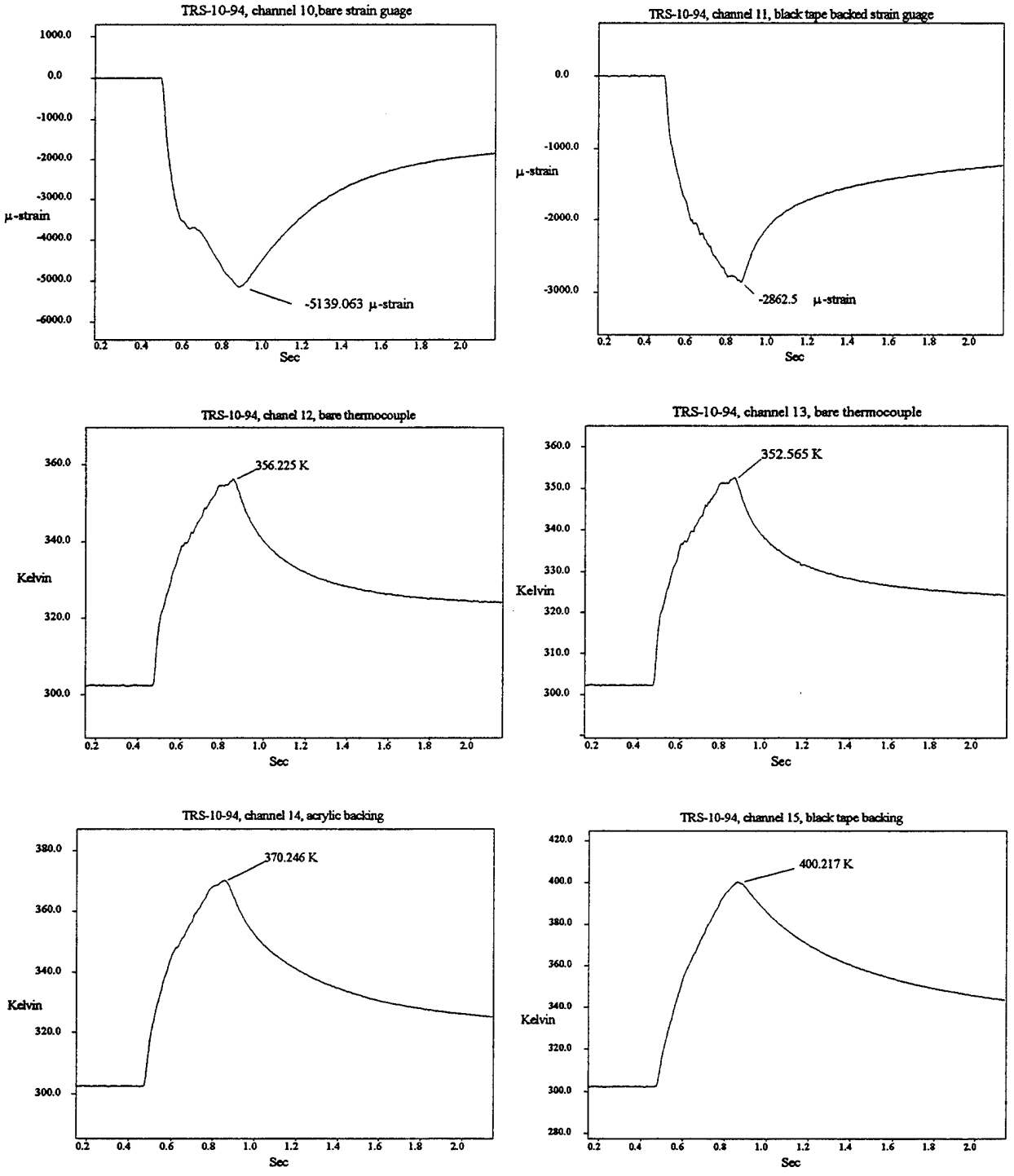

Figure 23. Comparison of thermal radiation effect on each sensor.

As seen in Table 4, the longer term conductive effects on strain show a much smaller deviation between mounting types. There is no recognizable difference in the thermocouple measurements. The difference in the strain could be attributed to the location of the strain gage on the panel. The bare strain gage was placed closer to the panels edge, and possibly there was a combination of strain relief from the edge, as well as conductive cooling from the plate mount. The difference is consistent for each experiment.

4.2 Thermal Radiation Transmission

The final two experiments included a highly sensitive calorimeter which was also a Gardon-type gage. The calorimeter was placed behind the panel with 1 cm space between the calorimeter face and the back of the panel. This calorimeter was able to measure the amount of thermal radiation transmitting through the composite panel. The first experiment with this calorimeter, TRS-10-94, is shown in Figure 24.

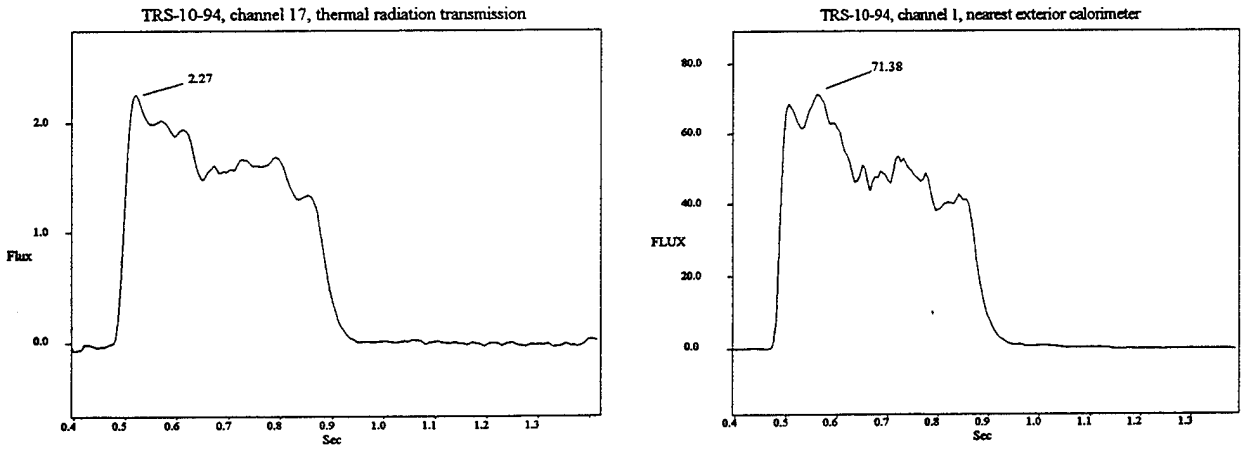

Figure 24. Thermal radiation transmission, TRS-10-94.

The peak thermal flux was 2.27 cal/cm^2-s, and the total fluence was 0.663 cal/cm^2. When compared to the data from channel 1, the panel allowed an average 3.09% of the radiant thermal energy to be transmitted.

4.3 Smoke Generation and Protection

The second transmission experiment, TRS-11-94, was conducted with the same composite panel used in TRS-10-94. A secondary objective was to determine the point at which smoke may be generated from the panel, and the degree to which it afforded protection from thermal radiation. Figure 25 shows the thermal radiation data of that experiment.

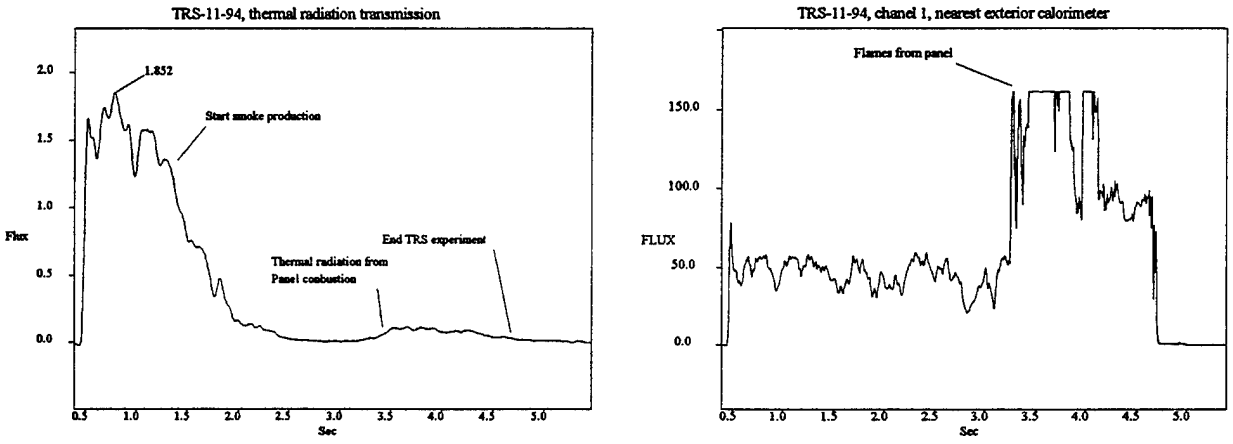

a) Thermal radiation transmission.

b) Incident thermal radiation on panel.

Figure 25. Thermal Radiation transmission, TRS-11-94.

The fluence measured by the calorimeter behind the panel was 1.88 cal/cm^2. The peak flux was 1.852 cal/cm^2-s. One can deduce from the data shown that smoke generation can fully protect a target from thermal radiation transmission. As seen in Figure 25a, in a little less than 1 s into the experiment, smoke from the panel began to obscure the transmission. During this time, the panel was allowing 3.87% of the thermal radiant energy through. About 0.5 s later, the level of thermal transmission had disappeared. At about 2.75 s into the experiment, the panel ignited and began to burn. Some of the energy produced by the combustion radiated through the panel, and amounted to about 0.2 cal/cm^2-s. Smoke continued to obscure the TRS energy until the end of the experiment.

The panel was completely destroyed after the experiment. It had ignited and burned. The flat profile at 150 cal/cm^2-s was due to the signal exceeding the band edge of the data recorder. The high levels were due to the panel combustion and the hot combustion products enveloping the calorimeter. No other calorimeter demonstrated this behavior, which eliminated the possibility of a TRS flare.

5. CONCLUSIONS

A simple problem in the instrumentation of composite materials has opened a question with regard to protection from thermal radiation effects. Obviously, thermal radiation can be transmitted through composite materials. The question is, To what degree is the equipment that the composite material is designed to protect affected? In the series of experiments discussed, the amount of energy being transmitted was relatively low. Some simple things could be done to reduce the amount of thermal radiation transmission, such as using thicker composite, injecting an opaque dye into the composite matrix material, or using surface coatings that produce heavy smoke when irradiated.

The answer to eliminating the thermal radiation transmission effect from sensors used to measure material response is left unknown. The effort of this experiment was to determine the cause of an unusual behavior in the early part of the data. This was done without any doubt, the cause being thermal radiation transmission through the composite which directly affected the sensor. How does one eliminate this from future work? This could be done by recognizing what the effect is and eliminating it from the data. This could prove to be extremely difficult in some cases and does not make for a sound experimental technique. Another method of eliminating this effect needs to be developed. Perhaps some form of radiation shielding that is similar to that used with thermocouples measuring air temperature in a room, where the walls are at a different temperature than the air, could be used. The shielding could be baked into the composite material with the thermocouple. This would also present certain disadvantages, such as being a potential point for delamination of the material when it is under stress.

Further research in this area is necessary to develop better methods of radiation compensation in semitransparent materials. A supply of composite materials and the use of the TRS facility at ARL would present a unique opportunity to conduct this type of investigation, to determine and design effective techniques of taking thermal radiation measurements of nonopaque materials.

6. REFERENCES

Chapman, A. J. Heat Transfer. 4th Edition, New York: McMillan Publishing Company, 1984.

Glasstone, S., and P. J. Dolan. The Effects of Nuclear Weapons. Department of the Army Pamphlet No. 50-3, Headquarters, Department of the Army, Washington, DC, March 1977.

Loucks, R. B. "TRSFT.BAS." A basic program to perform a Fourier transform of a function in time described by an ASCII table. U.S. Army Ballistic Research Laboratory, Aberdeen Proving Ground, MD, September 1988.

Loucks, R. B. "Thermal Radiation Simulator Characterization Methods for the Rectangular Pulse." BRL-TR-3148, U.S. Army Ballistic Research Laboratory, Aberdeen Proving Ground, MD, September 1990.

Loucks, R. B. "Optimization and Modification of a Thin Flame Thermal Radiation Source." Paper presented at the 12th International Symposium on Military Applications of Blast Simulation, Perpignon, France, September 1991.

Loucks, R. B., P. C. Muller, and R. Thane. "Rebuilding and Modeling of a Thermal Radiation Source." ARL-TR-501, U.S. Army Research Laboratory, Aberdeen Proving Ground, MD, August 1994.

Intentionally left blank

APPENDIX A: PARABOLIC INTERPOLATION OF DATA

The method of deriving a reasonable estimate of contour lines depends on a few conditions: the predictability of the phenomenon outside the data set, the extent of extrapolation or interpolation, and the rationale for conducting the extrapolation or interpolation. Interpolation here means predicting a value or quantity of a point within a region bounded by two or more given points. Extrapolation means predicting the value of a point outside that region encompassed by two or more given points. Experimenters and theorists tend to favor the reliability of an interpolated value rather than an extrapolated value. In the case of TRS experimentation, such interpolation and extrapolation is sensible and reasonably reliable as a true estimate of TRS performance.

Typically, experimenters have performed such interpolations and extrapolations in a linear fashion. It can be argued that the data between given points is unknown, and a linear approximation is the best estimate possible with the given data. Linear interpolation and extrapolation is much simpler to perform than any other method. Usually, there are only two given points upon which to base a region's behavior. To perform a parabolic interpolation, one must have, as a minimum, three given points in a line. These points can define a parabola along that line. Interpolation and extrapolation occurs along the defined parabola. An example of this is demonstrated with the data from a TRS event.

First the test site is mapped out for lines of curve fitting. Figure A-1 shows the 2.44-m shock tube mock-up cross section with a 14 calorimeter array.

Spacing between the calorimeters (with the exception of 9) was 50 cm. The center calorimeter was placed in the center of the tube. Numbers along the ordinate and abscissa indicate each calorimeter's height and horizontal displacement with respect to the TRS nozzle top center. Nine of the calorimeter's data points are used to generate the parabolic curve fit. The remaining five points are for comparisons between data and estimates. Calorimeter 9 is an interpolated value, where calorimeters 12, 13, 14, and 15 will test extrapolation. The data are from TRS-03-92, the third TRS experiment performed at ARL in 1992. Table A-1 lists the data results.

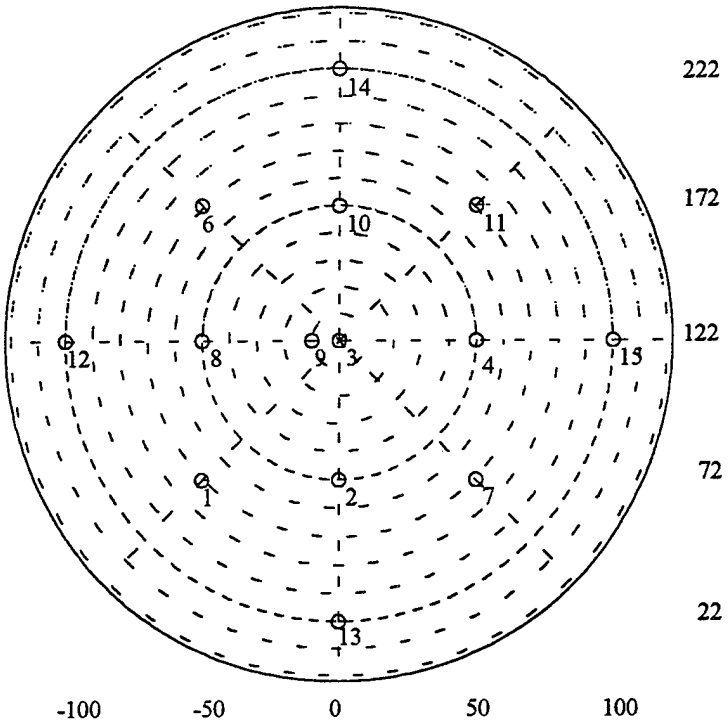

Figure A-1. Area of consideration in 2.44-m shock tube mock-up.

Table A-1. TRS-3-92 data

Calorimeter	Spatial Position	Average Flux, cal/cm^2-s	Fluence, cal/cm^2
1	-100/-50/72	34.72	31.07
2	-100/0/72	41.64	39.85
3	-100/0/122	43.95	38.96
4	-100/50/122	31.16	25.68
5	100/0/122 ST	34.30	36.65
6	-100/-50/172	33.88	27.46
7	-100/50/72	21.71	21.37
8	-100/-50/122	25.91	29.64
9	-100/-10/122	45.11	42.32
10	-100/0/172	45.01	32.76
11	-100/50/172	35.65	25.08
12	-100/-100/122	19.60	16.89
13	-100/0/22	36.31	35.48
14	-100/0/222	25.71	21.37
15	-100/100/122	9.46	9.49

Any combination of three calorimeters in a line can be considered. Take the line consisting of calorimeters 2, 3, and 10. Using the fluence values, the technique is to fit into a parabola of the form

$$y = Ax^2 + Bx + C, \tag{A-1}$$

where y are the point values (fluence), and x is the distance along the line.

To simplify the procedure, use the value at calorimeter 3 at the abscissa origin. Table A-2 lists the three values used to solve for the remaining constants A, B, and C.

Table A-2. Parabolic Fit Point Values

n	x_n	y_n
1	-50 cm	39.85 cal/cm^2
2	0 cm	38.96 cal/cm^2
3	50 cm	32.76 cal/cm^2

A, B, and C are solved simply by substituting the values of Table A-2 into equation A-1 as follows:

$$A = \frac{y_1 - Bx_1 - C}{x_1^2},$$

$$B = \frac{\left[C\left(x_1^2 - x_3^2\right) + x_3^2 y_1 + x_1^2 y_3\right]}{x_1 x_3 (x_3 - x_1)}, \tag{A-2}$$

$$C = y_2.$$

The value for **C** becomes the center point value, or 32.64 cal/cm^2. In this case, the constants are solved as

$$A = 1.062 \times 10^{-3},$$
$$B = -0.0709,$$
$$C = 38.96.$$

A compilation of the values from Table A-1, using the procedure described results in Table A-3. Note that the distance between calorimeters 6 and 3 and that of all diagonal distances are 70.7 cm, not 50 cm.

Table A-3. Solutions for Parabolic Constants

Calorimeter Combination	A	B	C
1, 8, 6,	-1.5×10^{-4}	-0.0361	29.64
2, 3, 10,	1.062×10^{-3}	-0.0709	38.96
7, 4, 11,	-9.66×10^{-4}	0.0371	25.64
6, 10, 11	-2.596×10^{-3}	-0.0238	32.76
8, 3, 4	-4.52×10^{-3}	-0.0396	38.96
1, 2, 7,	-5.452×10^{-3}	-0.097	39.85
6, 3, 7,	-5.815×10^{-3}	-0.0609	38.96
1, 3, 11,	-4.354×10^{-3}	-0.0599	38.96

Using the interpolated parabolic equations for the lines of interest, incremental values of fluence can be located on the map of Figure A-1. An example is to find the points along the lines where the fluence is exactly 20 cal/cm^2. This can be done by using the quadratic equation

$$x = \frac{-B \pm \sqrt{B^2 - 4AC + 4Ay}}{2A}, \qquad \text{(A-3)}$$

where y is given as 20 cal/cm^2. Table A-4 list the resulting locations of the desired fluence points along the map lines.

Table A-4. Location of Specified Fluence Along Map Points

Calorimeter Combination	x values for 20 cal/cm^2
1, 8, 6,	-400.95, 160.28
2, 3, 10,	-171.1, 104.34
7, 4, 11,	-59.58, 97.99
6, 10, 11	-74.8 65.68
8, 3, 4	-69.29, 60.54
1, 2, 7,	-69.88, 52.10
6, 3, 7,	-62.55, 52.10
1, 3, 11,	-73.23, 59.47

The values are plotted on the map, as shown in Figure A-2. The points of extrapolation are shown connected with a straight line but can be connected with a smooth curve.

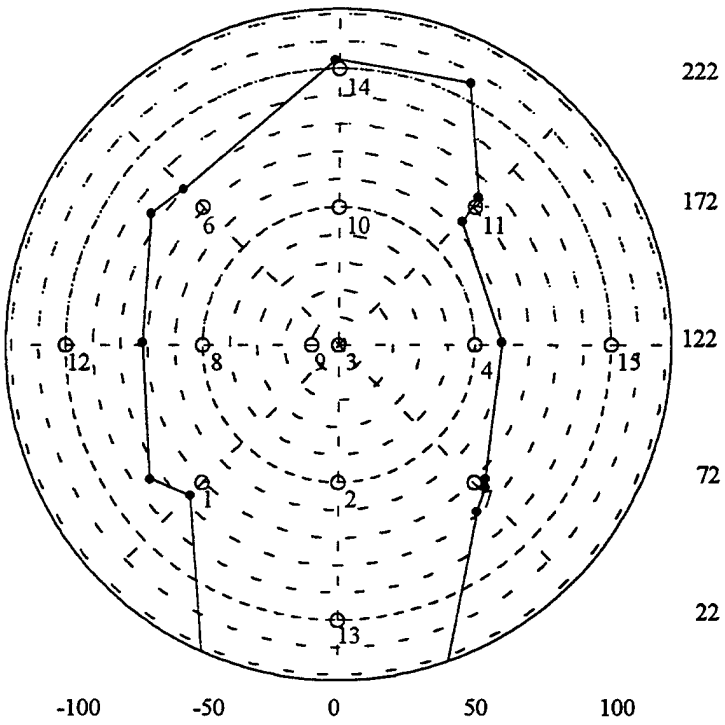

Figure A-2. Thermal mapping of isoradiance, linear connection.

The same procedure can be used for other fluence levels, average flux, or any other parameters used to evaluate the effect of the TRS in an environment of concern.

Intentionally left blank

APPENDIX B: PLOTS OF DATA

The TRS data are presented on the page in the same relative location as they would appear on the array. The top left plot, channel 5, was the top left calorimeter facing away from the TRS source. The standard calorimeter was placed on the opposite side of the TRS and remained in that spot for all experiments and pre-experimental tests; its spatial location is given as 100/0/30. Interpolated value is a weighted average of calorimeter data from channels 1, 2, 3, and 9. The weighting was determined from the proximity of the desired point to the location of the calorimeter. The calorimeter data at a certain point in time were multiplied by the linear distance to the point, then summed with the other distance-data products. The summation was divided by the total length of the distances used.

The response data are first shown in their entirety, then in extracted form. Recorder sample rate was 200 Hz. The comment on the plot which reads, "Extract(W1,50,400)" means "From window 'W1', eliminate the first 50 points, and plot the next 400 points." The 400 points would represent a window of 2 s. A blank space, or block, indicates no data were obtained at that point. The abbreviations "tc" and "sg" mean thermocouple and strain gage, respectively.

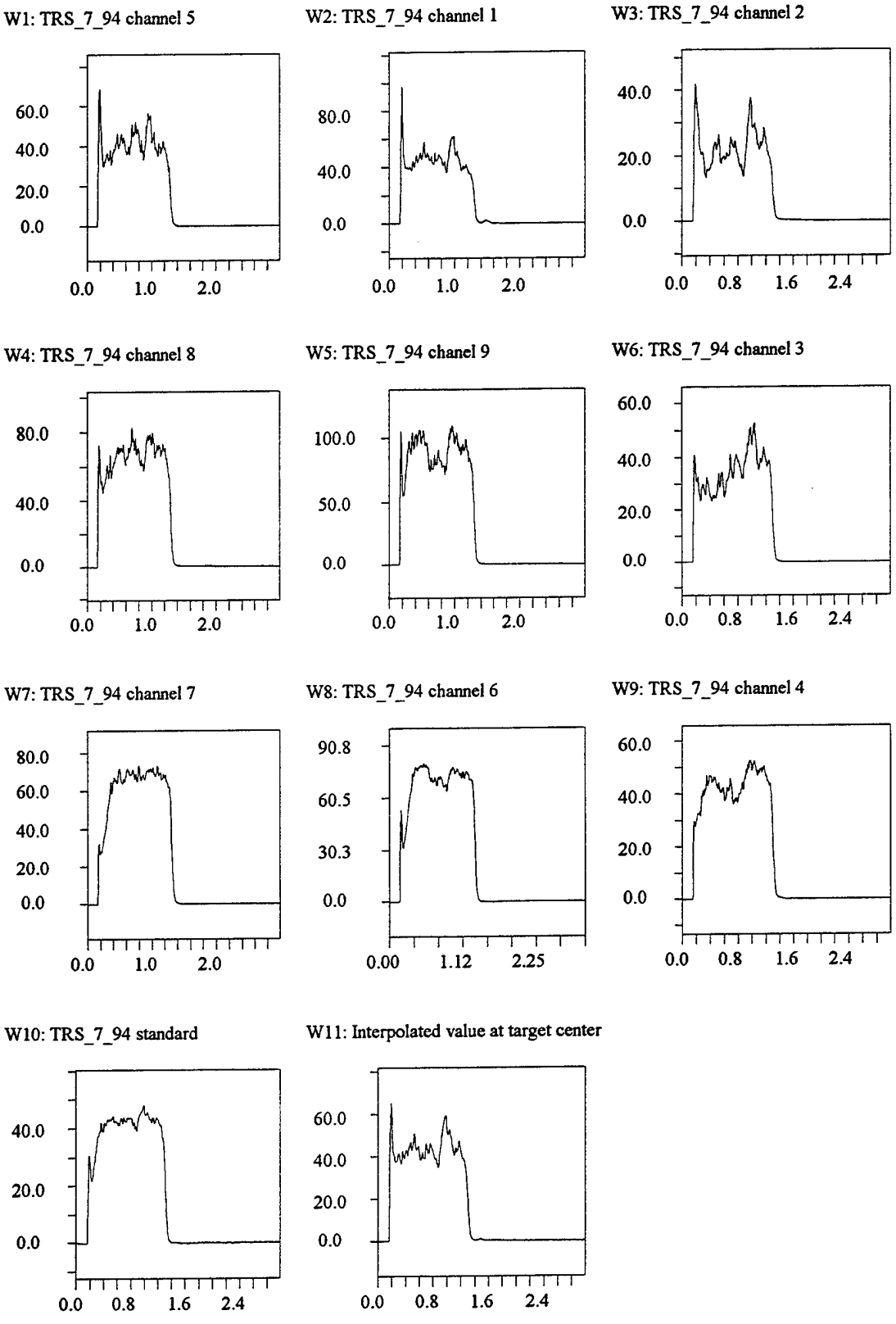

Figure B-1. TRS data from TRS-7-94.

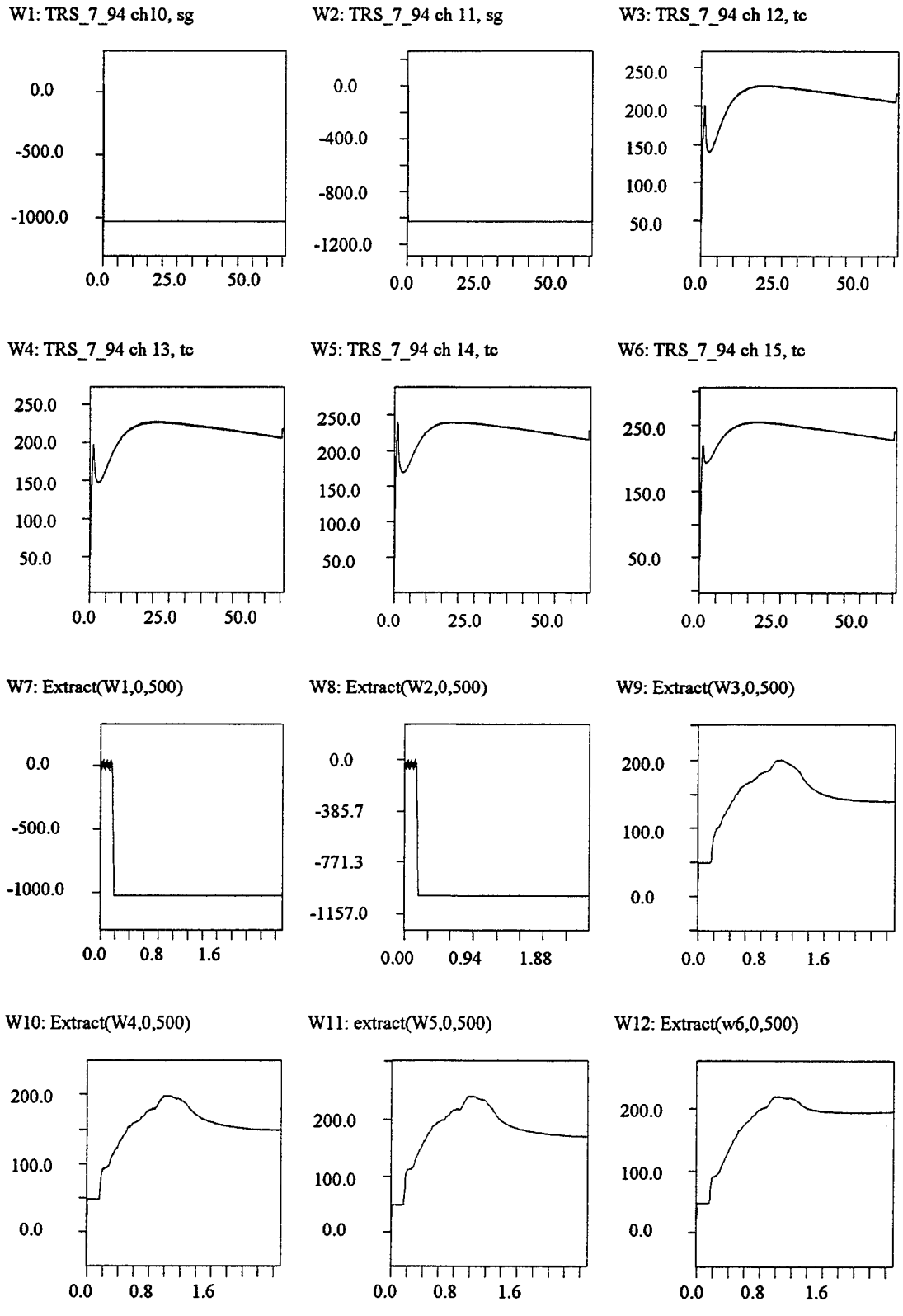

Figure B-2. Sensor data, TRS-7-94.

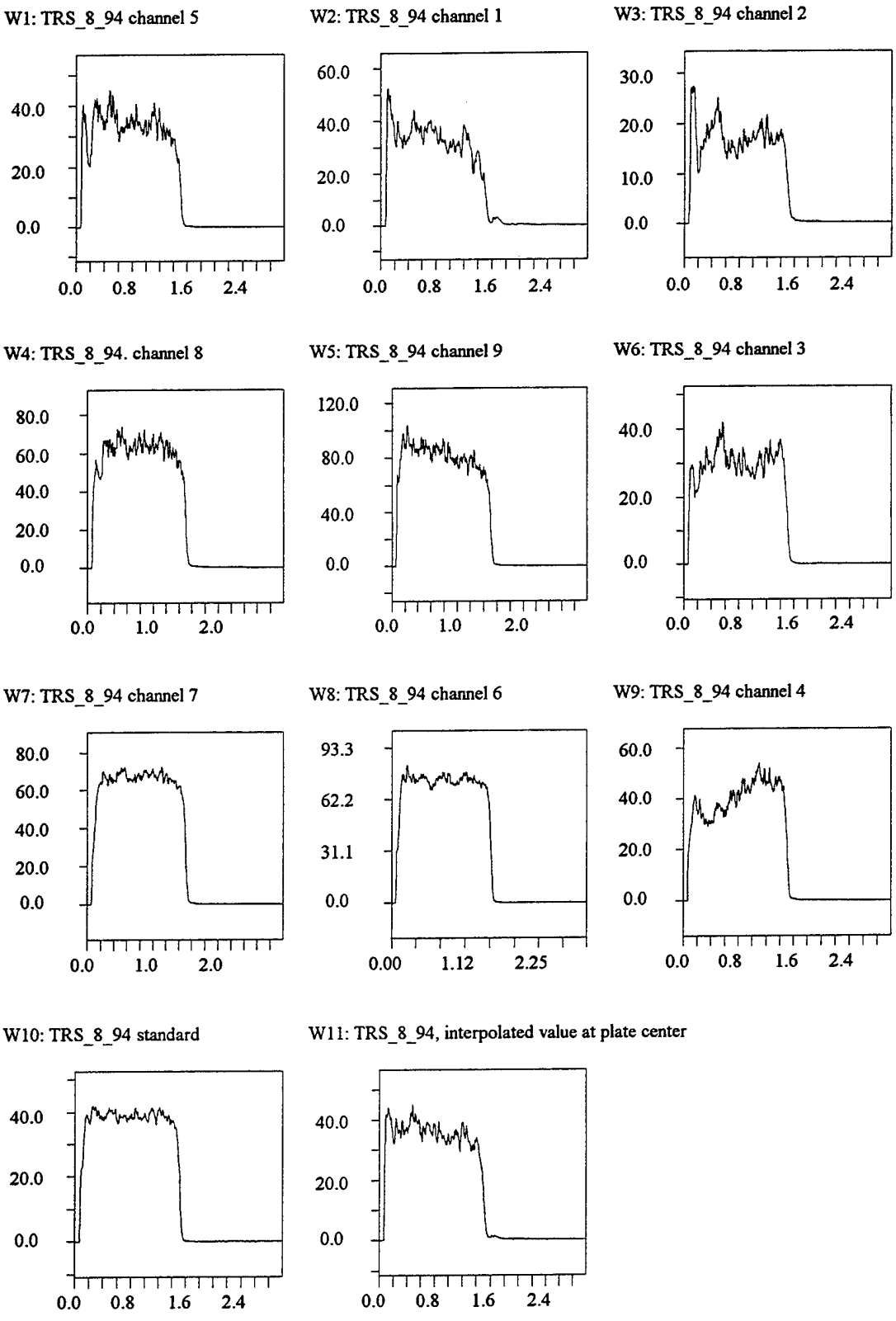

Figure B-3. TRS data from TRS-8-94.

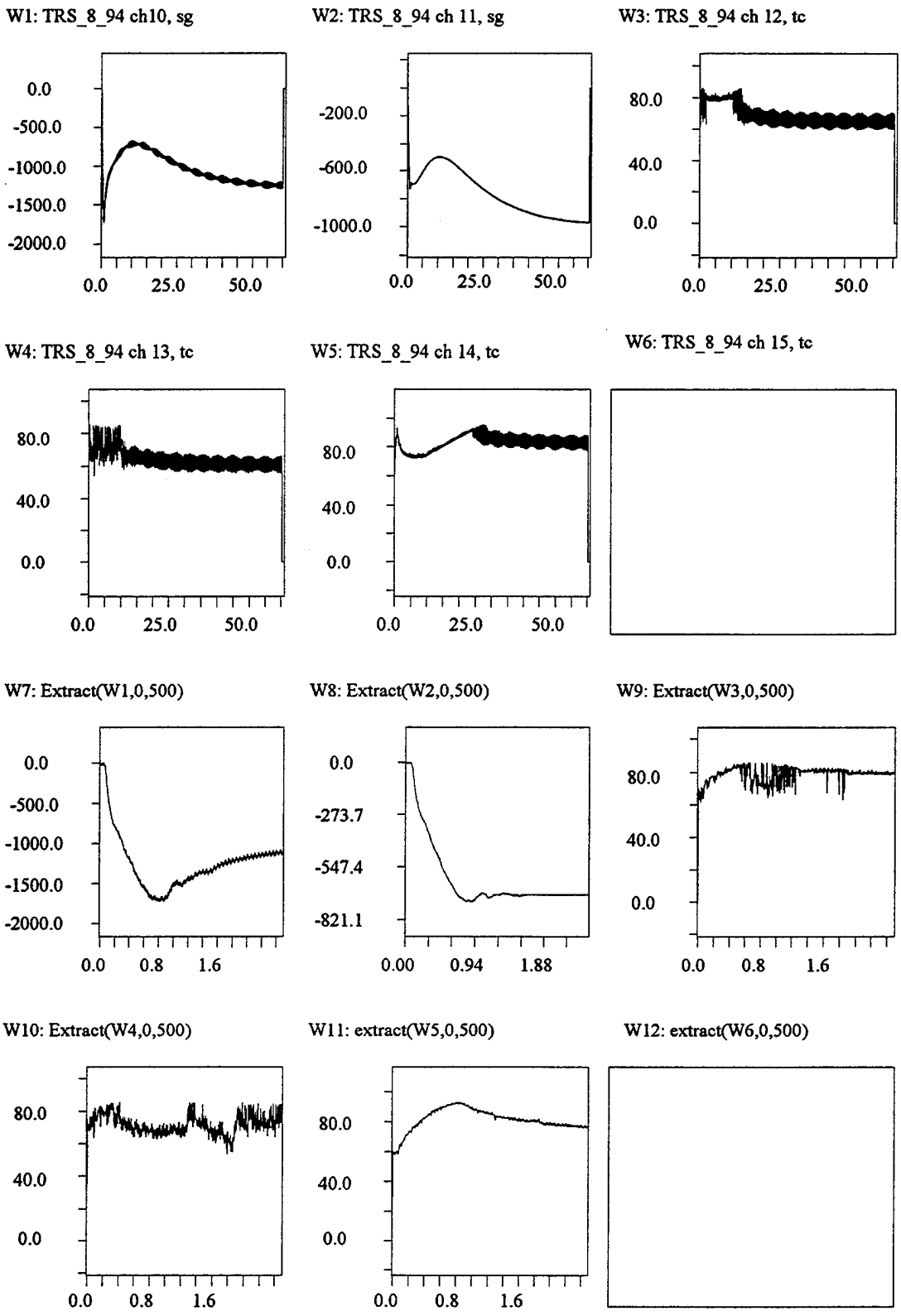

Figure B-4. Sensor data, TRS-8-94.

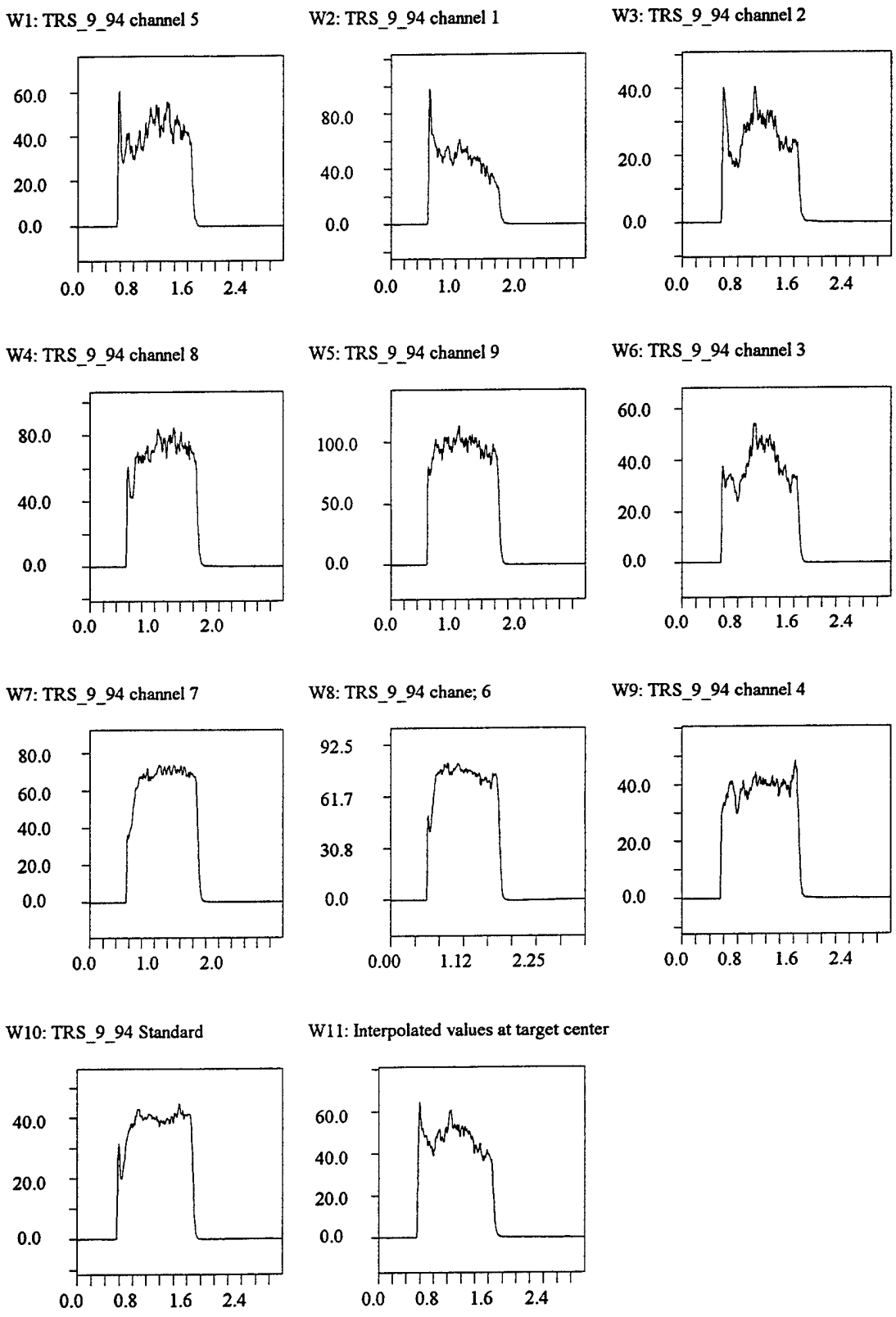

Figure B-5. TRS data from TRS-9-94.

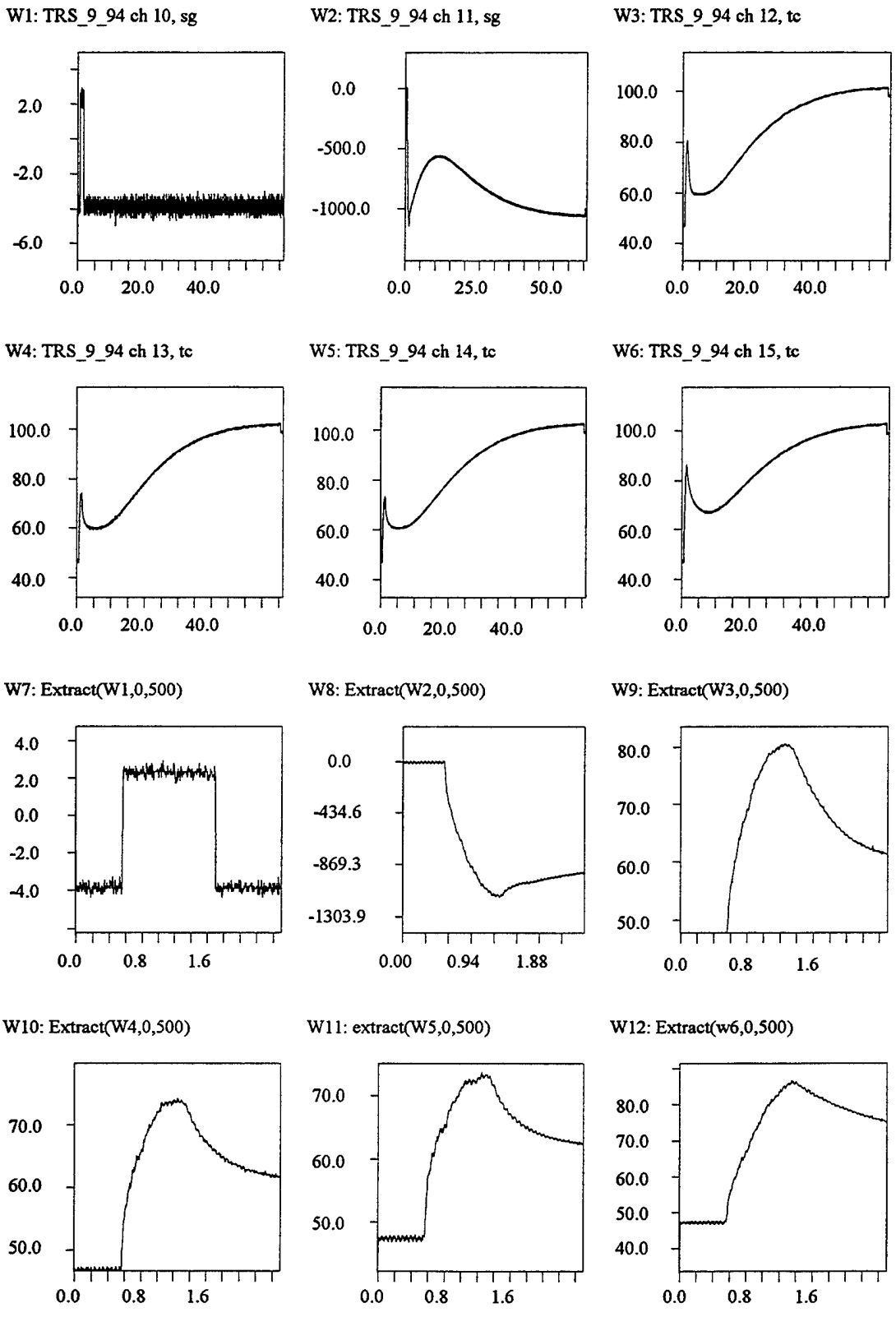

Figure B-6. Sensor data, TRS-9-94.

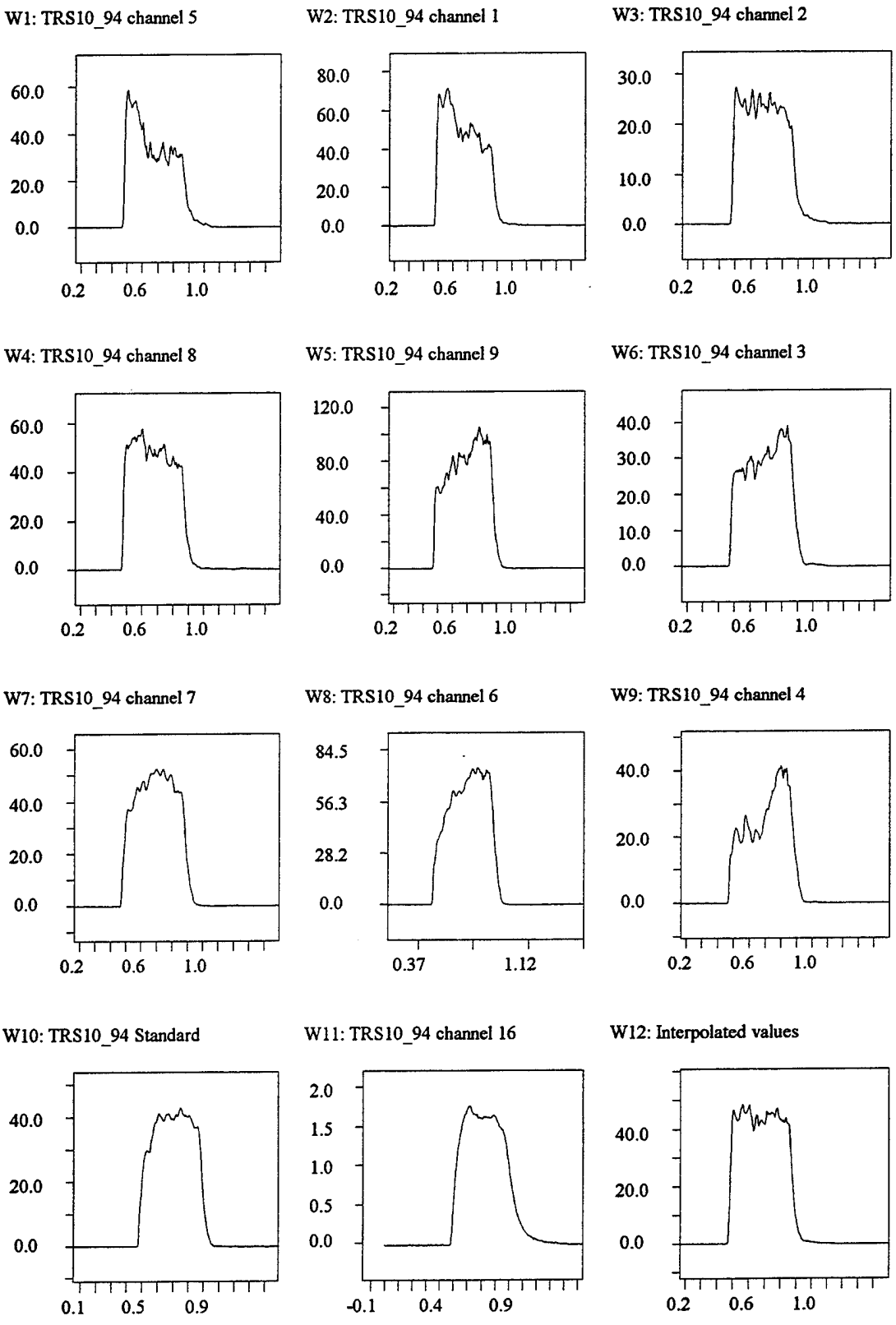

Figure B-7. TRS data from TRS-10-94.

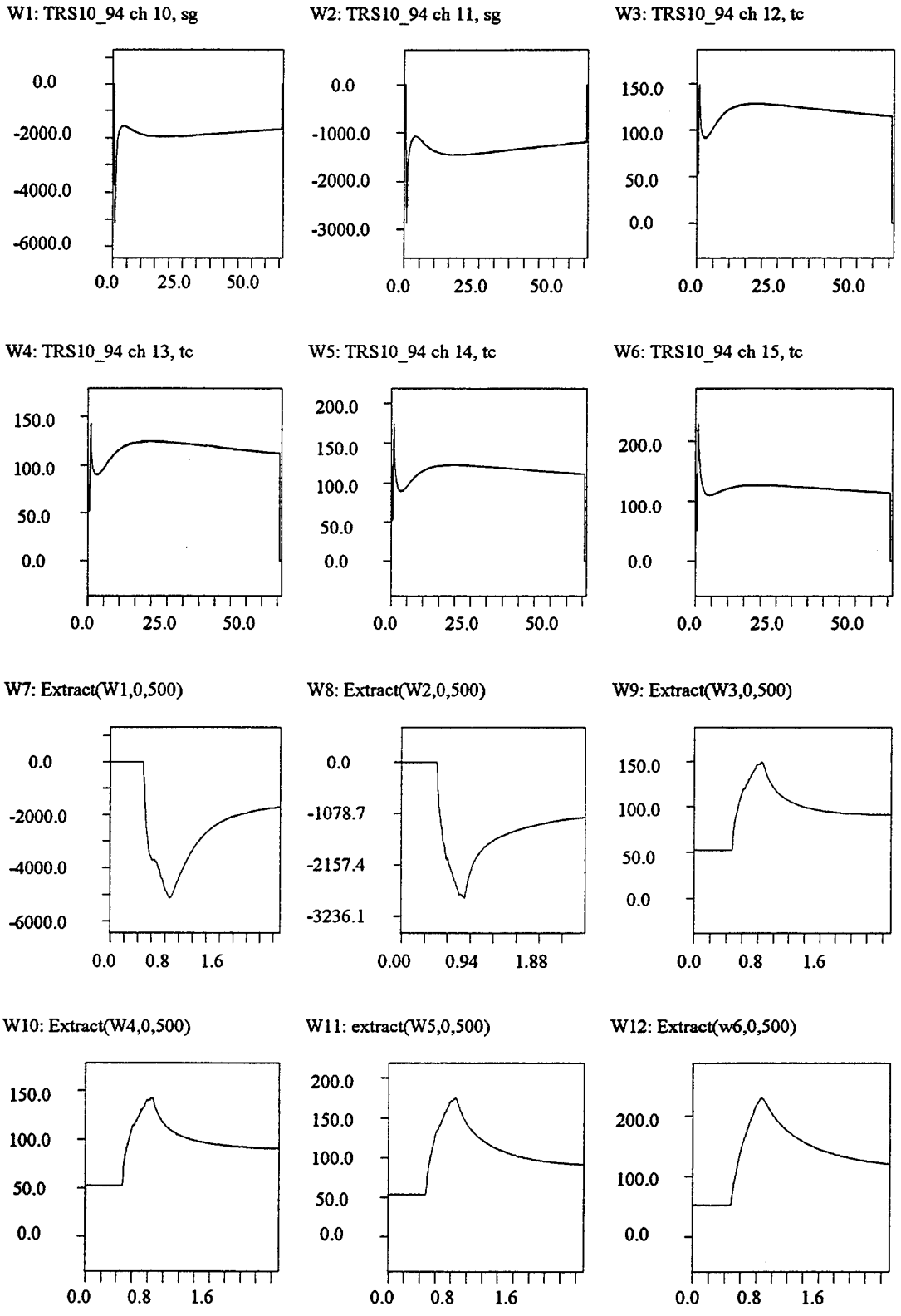

Figure B-8. Sensor data, TRS-10-94.

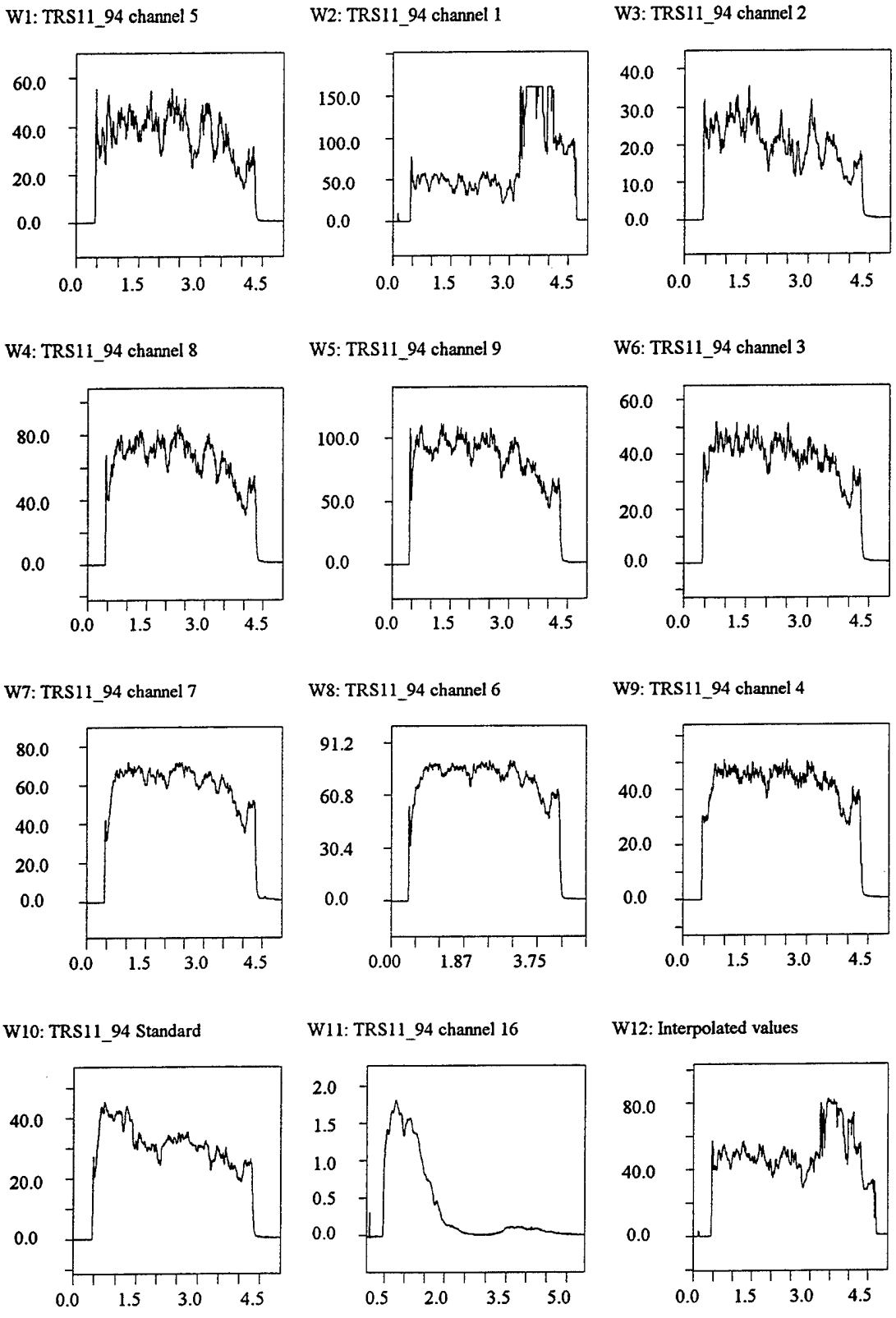

Figure B-9. TRS data from TRS-11-94.

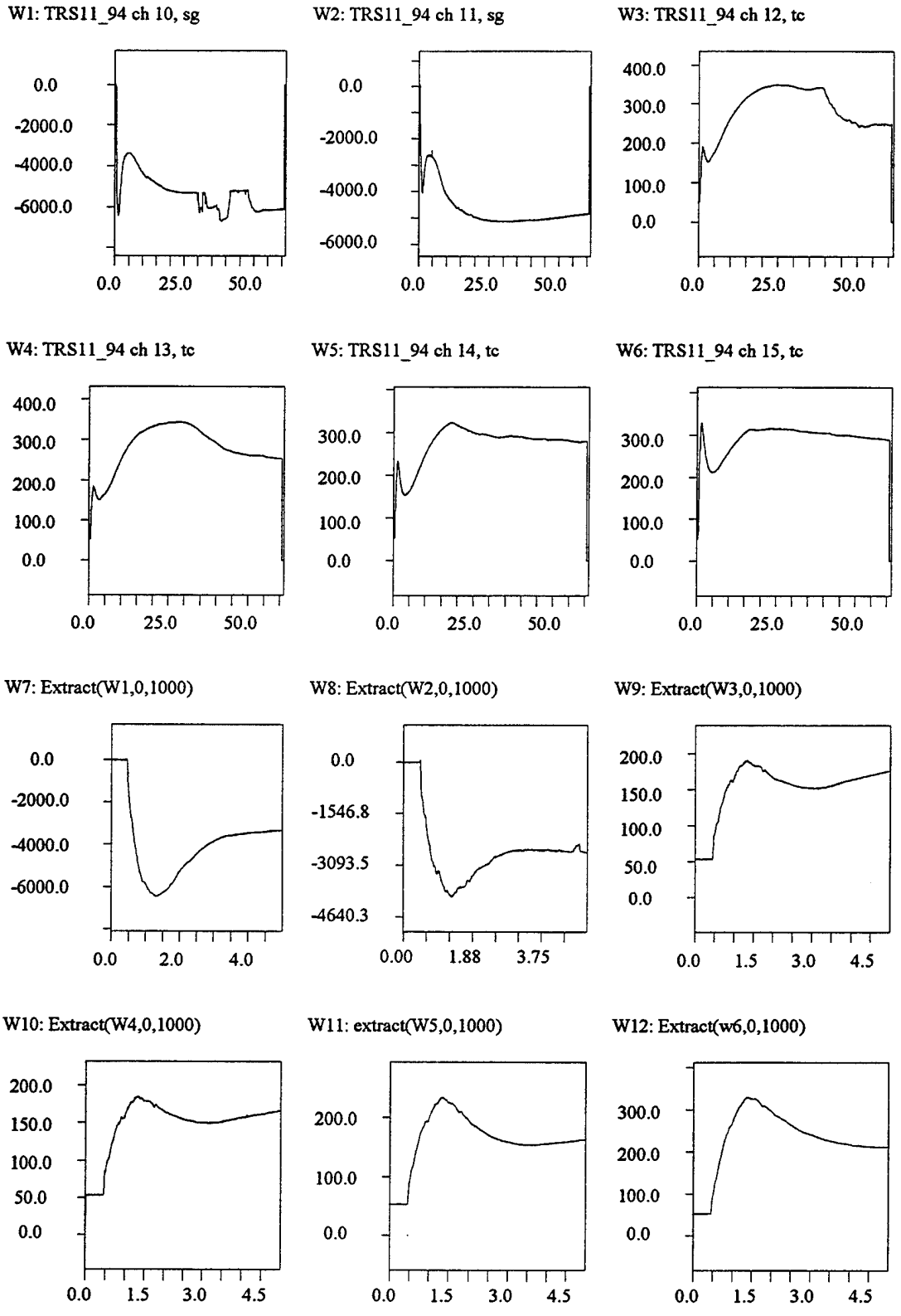

Figure B-10. Sensor data, TRS-11-94.

Intentionally left blank

APPENDIX C: CONTOUR PLOTS OF TRS DATA

The contour plots presented in this section were derived from a topography smoothed by using a cubic spline interpolation of five additional points between the actual calorimeter points. Five interpolated values were selected because there were no appreciable changes when using a greater number of interpolation points. The actual calculation was done automatically using MATHCAD 5.0 PLUS software on **Microsoft Windows Work Group** V3.11 on an IBM-compatible personal computer.

The corners of the plot, the ends of the grid lines, and the center are the calorimeter locations. Refer to Table 2 for the numerical values at these points. The contour plots clearly show the point of highest thermal emission is near (-14, 48). Where the interpolated points are not data, it is fair to say they represent the continuous topography in a better fashion than no interpolation. The first contour plots demonstrate this in Figure C-1. The contour lines are smooth, and most likely demonstrate the average flux during the event. Figure C-2 is the same data shown as a surface plot. Again, the interpolated surface is a more likely representation of the average flux during that experiment. Figures C-3 through C-7 show contours of constant flux and fluence. The values are all in calories/square centimeter-second and calories/square centimeter, respectively.

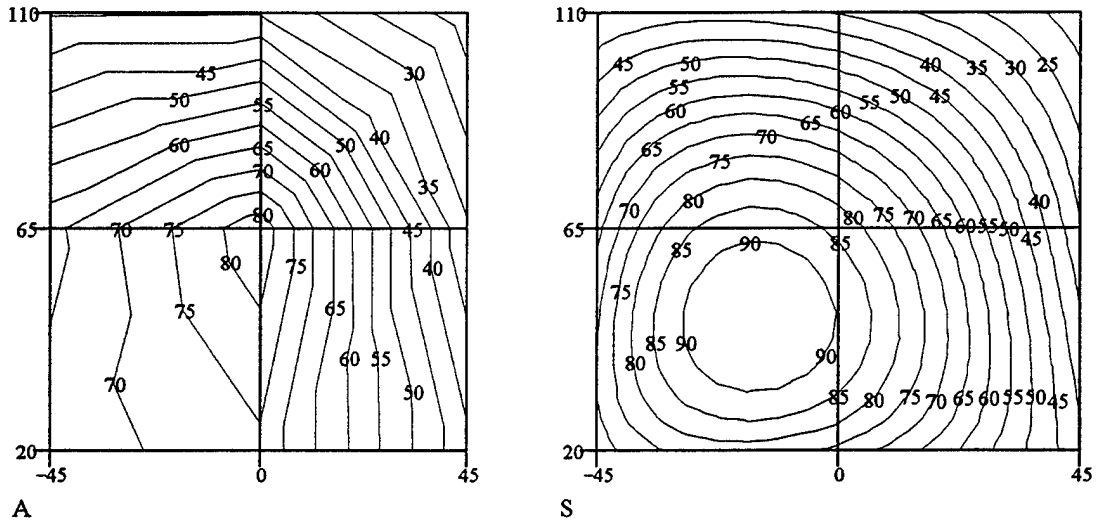

a) Data only

b) Data with interpolated result

Figure C-1. Comparison of contour plot results, flux of TRS-8-94.

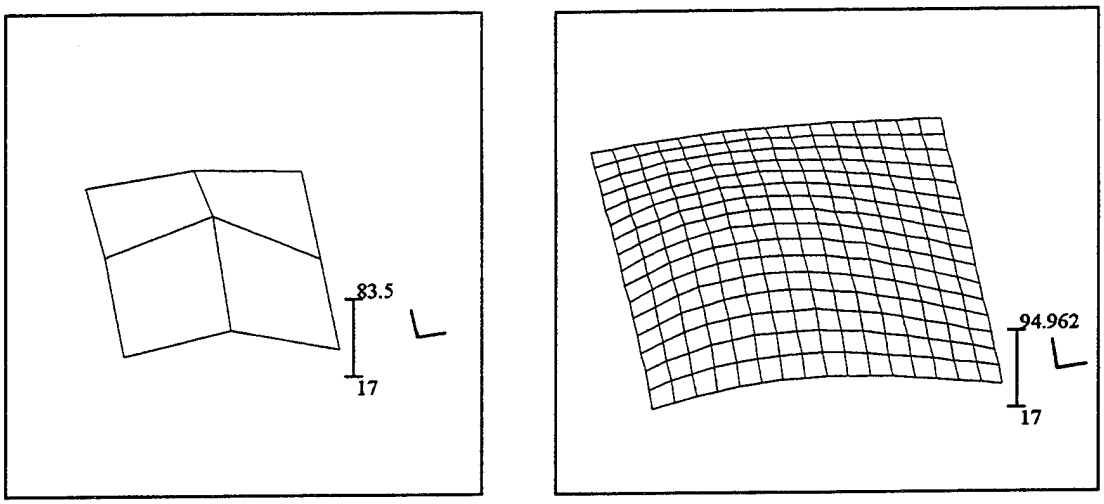

a) Data only

b) Data with interpolated "data"

Figure C-2. Comparison of topographical map, flux of TRS-8-94.

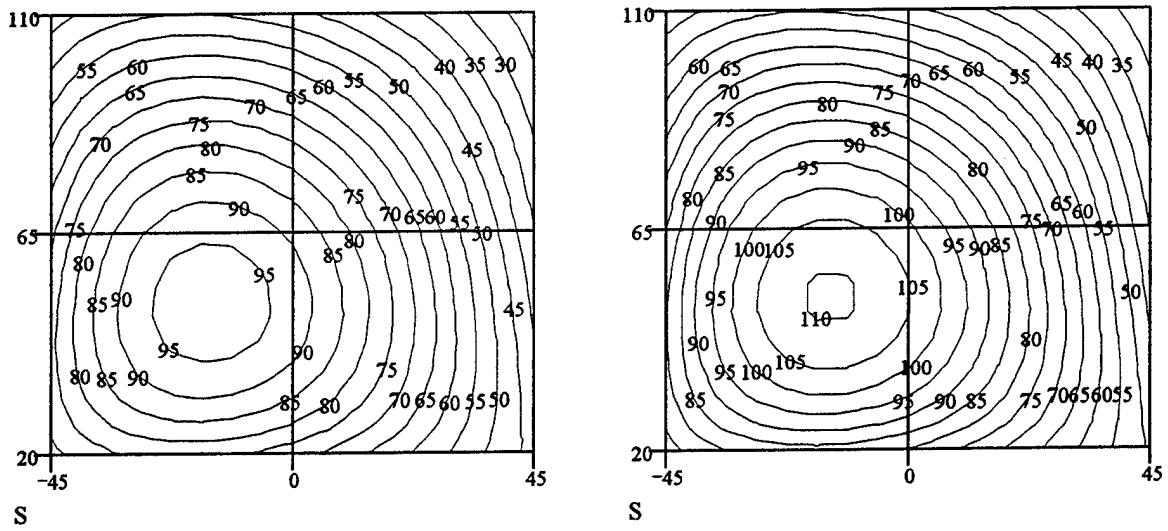

a) Flux

b) Fluence

Figure C-3. TRS-7-94.

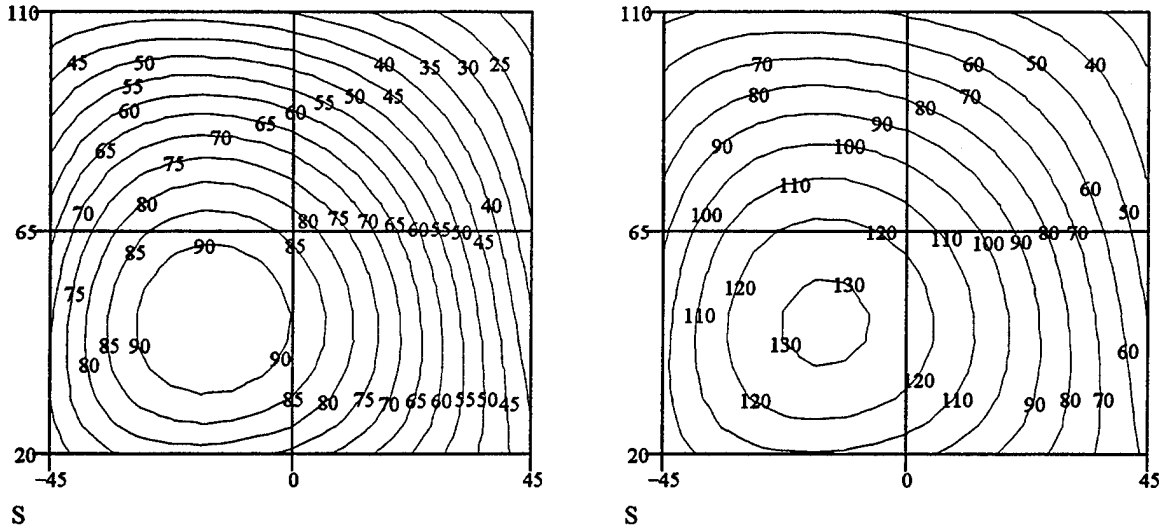

a) Flux b) Fluence

Figure C-4. TRS-8-94.

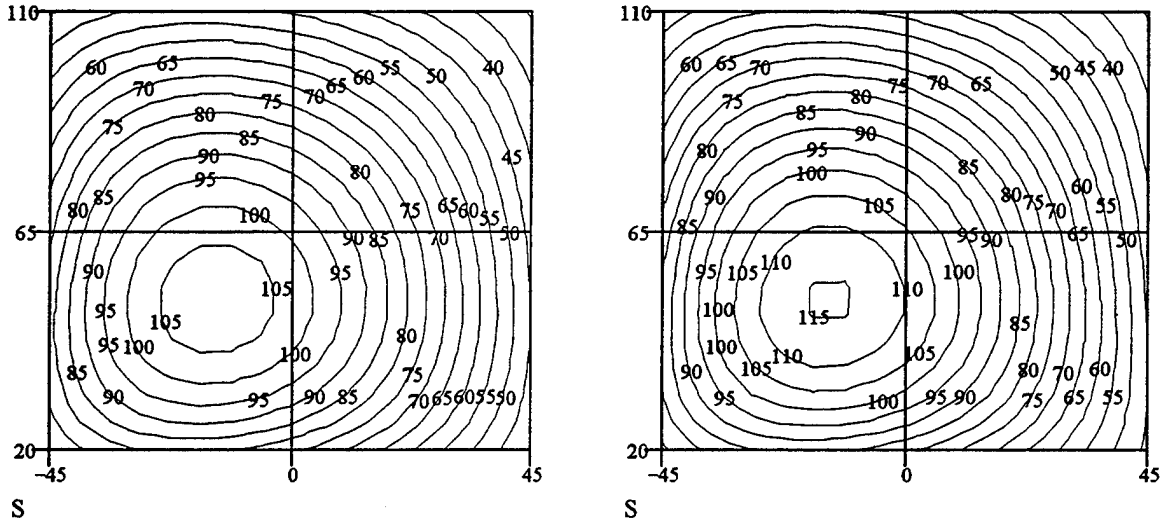

a) Flux b) Fluence

Figure C-5. TRS-9-94.

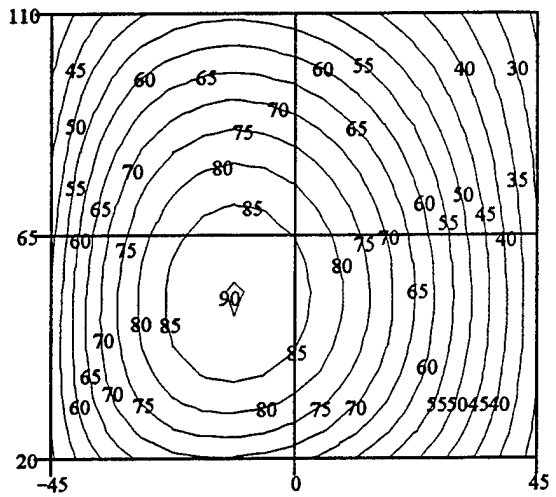

a) Flux

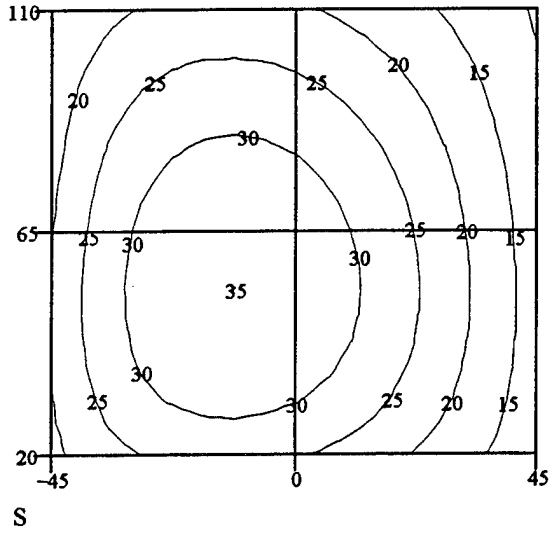

b) Fluence

Figure C-6. TRS-10-94.

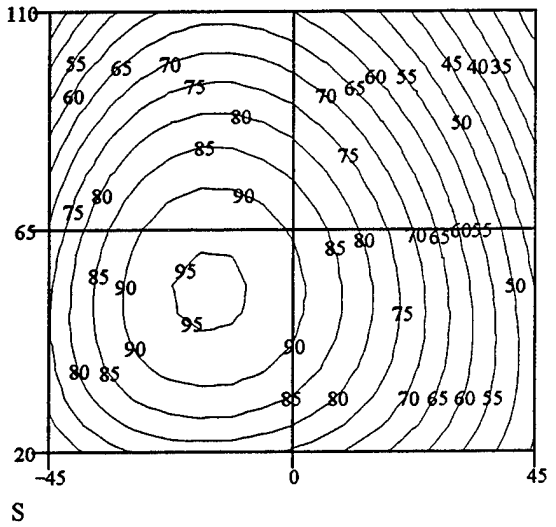

a) Flux

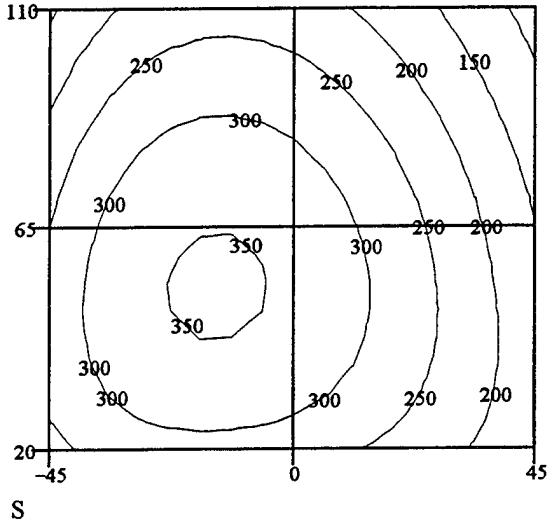

b) Fluence

Figure C-7. TRS-11-94.

NO. OF COPIES	ORGANIZATION
2	ADMINISTRATOR ATTN DTIC DDA DEFENSE TECHNICAL INFO CTR CAMERON STATION ALEXANDRIA VA 22304-6145
1	DIRECTOR ATTN AMSRL OP SD TA US ARMY RESEARCH LAB 2800 POWDER MILL RD ADELPHI MD 20783-1145
3	DIRECTOR ATTN AMSRL OP SD TL US ARMY RESEARCH LAB 2800 POWDER MILL RD ADELPHI MD 20783-1145
1	DIRECTOR ATTN AMSRL OP SD TP US ARMY RESEARCH LAB 2800 POWDER MILL RD ADELPHI MD 20783-1145
	ABERDEEN PROVING GROUND
5	DIR USARL ATTN AMSRL OP AP L (305)

NO. OF COPIES	ORGANIZATION
2	UNDER SECRETARY OF DEFNS FOR RSRCH AND ENGRG ATTN TWP OM T HITCHCOCK WASHINGTON DC 20301-3100
2	DIR ATTN TECH LIB T HAFNER DEFNS ADVNCD RSRCH PROJ AGCY 3701 N FAIRFAX DR ARLINGTON VA 22203-1714
1	DIR ATTN TECH LIB DEFNS INTLLGNC AGCY WASHINGTON DC 20301
7	CDR ATTN T KENNEDY C MCFARLAND C GALLAWAY E PATNAIK R ROHR G ULLRICH M HOLM DEFNS NUC AGCY WASHINGTON DC 20305-1000
1	HQDA ATTN DAEN RDZ A WASHINGTON DC 20310-1000
1	HQDA ATTN DAEN RDM WASHINGTON DC 20310-1000
1	HQDA ATTN SARD TR K KIMONOS WASHINGTON DC 20310-0103
1	HQDA ATTN SARD TR R CHAIT WASHINGTON DC 20310-1030
1	HQDA ATTN SARD TT C NASH WASHINGTON DC 20310-0103
1	HQDA ATTN SARD TT F MILTON WASHINGTON DC 20310-1030

NO. OF COPIES	ORGANIZATION
3	NATICK RD&E CTR ATTN F BISSETT PDS SATD STRNC YS KANSAS ST NATICK MA 01760-5020
2	CDR ATTN TECH LIB ATCD G M PASTEL US ARMY TRAINING & DOCTRINE CMND FT MONROE VA 23651
3	CDR ATTN SMCAR AEE WW PAI LU N SLAGG J PEARSON US ARMY ARMAMENT RD&E CTR PICATINNY ARSENAL NJ 07806-5000
10	CDR ATTN TECH LIB STRBE N HEBERLEIN STRBE NA WEAVER STRBE BLORE STRBE CFLO STRBE NE 3 CYS STRBE ND SPITZER STRBE NDM DILLON FT BELVOIR VA 22060-5606
14	DIR ATTN AMSRL SS FF J GERBER T PHAM M FONG K TRAN AMSRL WT N J GWALTNEY J INGRAM J MCGARRITY AMSRL WT NA R KEHS AMSRL WT NB M ABE AMSRL WT ND J MILETTA AMSRL WT NF L JASPER AMSRL WT NG T OLDHAM AMSRL WT HD J CORRIGAN AMSRL SL C J HUGHES US ARMY RESEARCH LABORATORY 2800 POWDER MILL RD ADELPHI MD 20783-1145

NO. OF COPIES	ORGANIZATION
3	DIR ATTN TECH LIB AMSRL MA PA W HASKELL E RIGAS US ARMY RESEARCH LABORATORY WATERTOWN MA 02172-0001
1	CDR ATTN STEW NED J MEASON US ARMY WSMR WSMR NM 88002
2	CDR ATTN TECH LIB AMFTA RSA T MEITZLER US ARMY TACOM WARREN MI 48397-5000
3	CDR ATTN TECH LIB G LONG D BACH US ARMY NUC AND CHEML AGCY 7150 HELLER LOOP STE 101 SPRINFIELD VA 22150-3198
2	COMMANDER ATTN TECH LIB M OGORZALEK US ARMY CONCEPTS ANALYSIS AGCY 8120 WOODMONT AVE BETHESDA MD 20814
1	CDR ATTN TECH LIB US ARMY RSRCH OFC PO BOX 12211 RSRCH TRI PK NC 27709
3	CDR ATTN T REEDER G GOODWIN TECH LIB US ARMY NGIC 220 7TH ST NE CHARLOTTESVILLE VA 22901-5396

NO. OF COPIES	ORGANIZATION
1	CDR ATTN TECH LIB US ARMY DUGWAY PROVING GROUND DUGWAY UT 84022
2	US ARMY CORPS OF ENGRS ATTN TECH LIB C HERRING CONST ENGRG RSRCH LAB PO BOX 9005 CHAMPAIGN IL 61826-9005
8	US ARMY ENGR WATERY EXPERMT STAT ATTN TECH LIB J STOUT J INGRAM R DINAN G MCMAHON P KING C JOACHIM B ARMSTRONG PO BOX 631 VICKSBURG MS 39180-0631
1	CMDT ATTN TECH LIB US ARMY ENGINEER SCHOOL FT LEONARD WOOD MO 65473
1	CDR ATTN TECH LIB US ARMY COLD REGIONS R&E LAB PO BOX 282 HANOVER NH 03755
2	CDR ATTN STEYT MT EA C HASTON STEYT MT AT A HOOPER US ARMY YUMA PROVING GROUND YUMA AZ 85365
1	CDR ATTN R FRANSEEN US AMCOM FIELD ASST IN SCI AND TECHLGY PROG FT BELVOIR VA 22060-5606

NO. OF COPIES	ORGANIZATION
1	US ARMY CORPS OF ENGINEERS ATTN D NEBUDA OMAHA DISTRICT MAIL CODE CEMRO ED SH 215 N 17TH ST OMAHA NE 68102-4978
8	OFFICER IN CHARGE ATTN TECH LIB F WARNOCK R FERGUSON K CHIEN J COLLINS CODE R 45 R PERSH M RUPPALT CODE R31 A LE NAVAL SURFACE WARFARE CTR 10901 NEW HAMPSHIRE RD SILVER SPRING MD 20903-5640
4	CDR ATTN TECH LIB L FONTENOT J BROWN CODE G72 J POWERS NAVAL SURFACE WARFARE CTR 17320 DAHLGREN RD DAHLGREN VA 22448-5000
2	CDR ATTN TECH LIB M ORR CODE 1101 NAVAL SURFACE WARFARE CTR PHILADELPHIA PA 19112-5083
2	CDR ATTN TECH LIB WILLIAM A SCHMIDT NAVAL RSRCH LAB WASHINGTON DC 20375
1	CDR ATTN TECH LIB NAVAL SURFACE WARFARE CTR SILVER SPRING MD 20903-5000

NO. OF COPIES	ORGANIZATION
1	CDR ATTN TECH LIB NAVAL SURFACE WARFARE CTR CHINA LAKE CA 93555-6001
1	OFFICER IN CHARGE ATTN TECH LIB NAVAL EOD FACILITY INDIAN HEAD MD 20640
3	CDR ATTN R DENTON MAJ CUTCHALL TECH LIB NAVAL COASTAL SYSTEMS CTR PANAMA CITY FL 32407
1	NAVAL WARARE ASSESSMENT CTR ATTN B HULET PO BOX 5000 NWAC CORONA CA 91718-5000
2	DIR ATTN TECH LIB J BRIONES NUCLEAR EFFECTS DIRECTORATE WSMR NM 88002
2	CDR ATTN D VAUGHN TECH LIB MARINE CORPS RD&E CMND QUANTICO VA 22134-5080
1	CDR ATTN AETT SA MR JEFF SMITH 7TH ARMY TRAINING COMMAND HQ 7TH ATC UNIT #28130 APO AE 09114
1	CDR ATTN AMXLS SA MR SCOTT KOHNKE US NATIONAL TRAINING CTR BLDG 502 FT IRWIN CA 92310

NO. OF COPIES	ORGANIZATION
1	CDR ATTN AMSTI RLO NTC HECTOR LOPEZ US ARMY STRICOM STRICOM LNO BLDG 130 PO BOX 10332 FT IRWIN CA 92310
1	CDR ATTN AFZF CS SA MR ROY J HOLLEY HQ III CORPS FT HOOD TX 76544-5056
1	DIR ATTN AMSRL SS SL JIM CHOPAK US ARMY RESEARCH LABORATORY 2800 POWDER MILL RD ADELPHI MD 20783-1197
2	US DEPT OF ENERGY ATTN TECH LIB KK 22 K SISSON WASHINGTON DC 20585
1	US MILITARY ACADEMY ATTN CAPT KEITH E MATTHEWS DEPT OF MATH SCI WEST POINT NY 10996
2	USIA WORLD NET ATTN TECH LIB J RYAN RM 2410 PATRICK HENRY BLDG 601 D ST NW WASHINGTON DC 20547
1	PHILLIPS LAB ATTN TECH LIB KIRTLAND AFB NM 87118-6008
5	FIELD COMMAND DNA ATTN LCDR Z MYERS CPT M SCOTT J RENICK E MARTINEZ 2 CYS KIRTLAND AFB NM 87115-5000
1	AFOSR ATTN TECH LIB BOLLING AFB DC 20332

NO. OF COPIES	ORGANIZATION
3	WL MNME ATTN G PARSONS J FOSTER TECH LIB EGLIN AFB FL 32542-5000
1	DIR NASA SCIENCE TECHL INTNAT FACLTY PO BOX 8754 BWI AIRPORT MD 21240
2	NOAA OCEANIC AND ATMOSPHERIC RSRCH ATTN CPT SMART W CALLENDER 1335 E W HWY SSMC3 MAILCODE R PDC SILVER SPRING MD 20910
1	OIR CSD CRB ATTN A M JONES RM 1413 OHB WASHINGTON DC 20505
1	DIR ATTN TECH LIB IDAHO NAT LAB PO BOX 1625 IDAHO FALLS ID 83415
1	DIR ATTN TECH LIB LOS ALAMOS NAT LAB PO BOX 1663 LOS ALAMOS NM 87545
4	DIR ATTN TECH LIB R OSTENSEN S SNYDER M SAGARTZ SANDIA NAT LABS PO BOX 5800 ALBUQUERQUE NM 87185

NO. OF COPIES	ORGANIZATION
2	DIR ATTN TECH LIB A KUHL LAWRENCE LIVERMORE NAT LAB PO BOX 808 LIVERMORE CA 94550
1	AAI CORPORATION ATTN TECH LIB PO BOX 126 HUNT VALLEY MD 21030-0126
2	ABERDEEN RESEARCH CENTER ATTN J KEEFER N ETHRIDGE PO BOX 548 ABERDEEN MD 21001
1	AEROSPACE CORPORATION ATTN TECH LIB PO BOX 92957 LOS ANGELES CA 90009
1	ALCAN POWDERS AND CHEMICALS ATTN TECH LIB PO BOX 290 ELIZABETH NJ 07207
3	ALLIED CONTRACTORS INC ATTN TECH LIB T CRAWFORD A SIMPSON 204 E PRESTON ST BALTIMORE MD 21202
1	ALUMINUM COMPANY OF AMERICA ATTN TECH LIB 1501 ALCOA BLDG PITTSBURG PA 15219
1	AMPAL ATTN TECH LIB PO BOX 31 FLEMINGTON NJ 08822

NO. OF COPIES	ORGANIZATION
2	ANSER MISSILE DIVISION ATTN TECH LIB R LEGINUS CRYSTAL GATEWAY 3 1215 JEFFERSON DAVIS HWY ARLINGTON VA 22202
1	APPLIED RESEARCH ASSOCIATES INC ATTN R FLOREY 2750 EISENHOWER AVE STE 104 ALEXANDRIA VA 22314
2	APPLIED RESEARCH ASSOCIATES INC ATTN R GUICE R HEYMAN 5941 S MIDDLEFIELD RD LITTLETON CO 80123
1	APPLIED RESEARCH ASSOCIATES INC ATTN J DRAKE 3202 WISCONSIN AVE VICKSBURG MS 39180
1	ATLANTIC RESEARCH CORPORATION ATTN TECH LIB 5390 CHEROKEE AVE ALEXANDRIA VA 22314
1	ATOMIZED METAL POWDERS INC ATTN TECH LIB 25 E 39TH ST NEW YORK NY 10016
1	BATTELE TWSTIAC 505 KING AVE COLUMBUS OH 43202-2093
1	BDM CORPORATION ATTN TECH LIB 7915 JONES BRANCH DR MCLEAN VA 22102
2	BOEING HELICOPTERS ATTN TECH LIB J COSGROVE PO BOX 16858 MS P30 07 PHILADELPHIA PA 19142-0858

NO. OF COPIES	ORGANIZATION
2	BOEING MILITARY AIRPLANE COMPANY ATTN TECH LIB R LORENZ PO BOX 7730 WICHITA KS 67277-7730
1	BOOZ ALLEN & HAMILTON INC ATTN TECH LIB CRTSTAL SQ 2 STE 1100 1725 JEFFERSON DAVIS HWY ARLINGTON VA 22202-4158
2	DENVER RESEARCH INSTITUTE ATTN TECH LIB L BROWN PO BOX 10127 DENVER CO 80210
2	DYNAMIC SCIENCE INC ATTN S ZARDAS P NEUMAN PO BOX N ABERDEEN MD 21001
2	ELECTROSPACE SYSTEMS INC ATTN TECH LIB S PAREKH PO BOX 831359 RICHARDSON TX 75083-1359
1	EMTEC SYSTEMS INC ATTN J LATTERY 4500 ANAHEIM AVE NE B6 ALBUQUERQUE NM 87113
1	ETHYL CORPORATION ATTN TECH LIB HOUSTON PLANT BOX 472 PASADENA TX 77501
1	FMC CORPORATION ATTN TECH LIB 1105 COLEMAN AVE SAN JOSE CA 95108
1	FRANKLIN RESEARCH CENTER ATTN TECH LIB BENJAMIN FRANKLIN PKY PHILADELPHIA PA 19103

NO. OF COPIES	ORGANIZATION
2	GENERAL SCIENCES INC ATTN TECH LIB M RILEY 655 S GRAVERS RD PLYMOUTH MEETING PA 19462
1	ITT RESEARCH INSTITUTE ATTN TECH LIB 10 W 35TH ST CHICAGO IL 60616
2	ITT AEROSPACE OPTICAL DIVISION ATTN TECH LIB K RUSTER 3700 E PONTIAC ST PO BOX 3700 FT WAYNE IN 46803
3	THE JOHNS HOPKINS UNIVERSITY ATTN TECH LIB T COUGHLIN J KOUROUPIS APPLIED PHYSICS LAB JOHNS HOPKINS RD LAUREL MD 20707
1	KAMAN SCIENCES CORPORATION ATTN F MCMULLAN 6400 UPTOWN BLVD STE 300E ALBUQUERQUE NM 87110
2	MARTIN MARIETTA AEROSPACE ATTN TECH LIB M BAUER PO BOX 179 DENVER CO 80201
2	MCDONNELL DOUGLAS CORPORATION ATTN TECH LIB C COREY BALLISTIC MISSILE DEFENSE 5301 BOLSA AVE HUNINGTON BEACH CA 92647
1	MEDTHERM CORPORATION ATTN LARRY JONES PO BOX 412 HUNTSVILLE AL 35804

NO. OF COPIES	ORGANIZATION
2	NEW MEXICO ENGRG RSRCH INST ATTN TECH LIB R ROBEY U OF NM ALBUQUERQUE NM 87131-1376
1	DEPARTMENT OF STATISTICS ATTN DR JAMES R THOMPSON RICE UNIVERSITY HOUSTON TX 77251-1892
2	OLIN ORDNANCE ATTN TECH LIB J KIBIGER PRODUCT MATERIAL CONTROL 10101 9TH ST N ST PETERSBURG FL 33716
2	REYNOLDS METALS COMPANY ATTN TECH LIB N KOOPMAN PLANT #3 4101 CAMP GROUND RD LOUISVILLE KY 40211
3	S CUBED MAXWELL LABS ATTN TECH LIB C NEEDHAM K SCHNIEDER ALBUQUERQUE NM 87131
1	SI DIVISION OF SPECTRUM 39 ATTN W SCHUMAN 8831 SATYR HILL RD STE 312 BALTIMORE MD 21234
2	SCIENCE APPLICATIONS INTNL CORP ATTN TECH LIB J BRYARS 11526 SORRENTO VALLEY RD STE A SAN DIEGO CA 92121

NO. OF COPIES	ORGANIZATION
4	SCIENCE APPLICATIONS INTNL CORP ATTN J SIMMONS J GUEST J DISHON P VERSTEEGAN PO BOX 1303 1710 GOODRICH DR MCLEAN VA 22102
1	SCIENCE APPLICATIONS INTNL CORP ATTN S DOERR 2109 AIR PK RD SE ALBUQUERQUE NM 87106
1	SIBERLINE MANUFACTURING CO INC ATTN TECH LIB PO BOX A LANSFORD PA 18232
2	SIMULA GOVERNMENT PRODUCTS INC ATTN TECH LIB W PERCIBALLI 10016 S 51ST ST PHOENIX AZ 85044-5299
1	SOUTHWEST RESEARCH INSTITUTE ATTN TECH LIB PO DRAWER 28510 SAN ANTONIO TX 78284
1	SRI INTERNATIONAL ATTN TECH LIB 333 RAVENSWOOD AVE MENLO PK CA 94025
2	TECH REPS INC ATTN F MCMULLEN B COLLINS 5000 MARBLE NE STE 222 ALBUQUERQUE NM 87110
1	TELEDYNE MCCORMICK SELPH ATTN C GARRISON PO BOX 6 HOLLISTER CA 95023-0006
1	TERA ATTN TECH LIB NM INSTITUTE OF TECHLGY SOCORRO NM 87801

NO. OF COPIES ORGANIZATION

1 THERMOGAGE INC
ATTN CHARLES BROOKLY
330 ALLEGHANY ST
FROSTBURG MD 21532

1 TRANSMET CORPORATION
ATTN TECH LIB
4290 PERIMETER DR
COLUMBUS OH 43228

1 US BRONZ POWDERS INC
ATTN TECH LIB
PO BOX 31
RT 202
FLEMINGTON NJ 08822

2 UNIVERSITY OF MD AT COLLEGE PK
DEPT OF MECHL ENGRG
ATTN ENME J WALLACE
U PIOMELLI
RM 2168
COLLEGE PK MD 20742-5121

1 UNIVERSITY OF MD AT COLLEGE PK
ATTN ENGRG AND PHYS SCI LIB
MATHEMATICS BLDG
COLLEGE PK MD 20742

5 WALCOFF AND ASSOCIATES INC
ATTN T TOYA
C PAQUETTE
C WALCOFF
W DEAL
R WALDEN
12015 LEE JACKSON MEM HWY #500
FAIRFAX VA 22033-3300

1 STRICOM
ATTN AMSTI MC L LAWRENCE
2350 RESEARCH PKY
ORLANDO FL 32826-3276

ABERDEEN PROVING GROUND

1 CMD, AMCCOM
ATTN: SMCAR-ACW (E3516)
WEAPONS SYSTEMS CONCEPT TEAM

NO. OF COPIES ORGANIZATION

9 DIR, USAMSAA
ATTN: AMSXB-GB, ABEL
AMXSY-S, CARROLL
AMXSY-GC,
B BRAMWELL
C EISSNER
L MEREDITH
W WIDERMAN
A WONG
LTC HASSELL
JTCG-ME, LAGRANGE

5 CMD, USACSTA
ATTN: STECS-AE-CL,
R. SCUTTI
D. GRIFFEN
STECS-AE-TL, BINDEL
STECS-AE-TH, WILEY
STECS-LI, R. HENDRICKSEN

4 DIR, ERDEC
ATTN: SCDRB-RTT,
L BICKFORD
S FUNK
G GOLDSMITH
I SWANN

1 CDR, USAOC&S
ATTN: TECH LIB

6 CDR, USATECOM
ATTN: AMSTE-SI-F
AMSTE-CL
AMSTE-EV-O
AMSTE-TA-F
AMSTE-ML
AMSTE-TE-V

NO. OF COPIES	ORGANIZATION
63	DIR, USARL ATTN: AMSRL-CI-S, A. MARK AMSRL-CP-TI, J. POLK AMSRL-SL, J. WADE (433) J. SMITH (433) AMSRL-SL-I, M. STARKS (433) AMSRL-SL-B, P. DEITZ (328) AMSRL-SL-BA, J. WALBERT (1068) AMSRL-SL-BG, A. YOUNG (433) AMSRL-SL-BS, D. BELY (328) AMSRL-SL-BV, J. MORRISSEY (247) W. BAKER (247) J. COLLINS (247) L. MOSS (247) W. WINNER (247) AMSRL-CI-C, M. TAYLOR AMSRL-WT-NC, R. LOTTERO R. LOUCKS (20 CYS) P. MULLER R. THANE J. SULLIVAN G. FERGUSON S. SCHRAML C. MERMAGEN A. MIHALCIN AMSRL-WT-TB, J. CONDON AMSRL-WT-TD, P. KINGMAN AMSRL-WT-W, C. MURPHY AMSRL-WT-WA, B. MOORE H. ROGERS F. BRANDON T. GORDON BROWN W. D'AMICO W. CLAY D. HEPNER M. HOLLIS R. MCGEE AMSRL-WT-WD, G. THOMSON AMSRL-WT-WE, J. TEMPERLEY W. JOHNSON J. THOMAS J. WITAS AMSRL-WT-WG, L. PUCKETT AMSRL-W-WC, J. ROCCHIO

NO. OF COPIES	ORGANIZATION
2	CDR, HRED ATTN: AMSRL-HR-SB, W. HANLON AMSRL-HR-SD, J. KALB

NO. OF COPIES ORGANIZATION

2 BUNDESAMT FÜR WEHRTECHNIK
UND BESCHAFFUNG
ATTN: K KÖHLER
TECH LIB
POSTFACH 7360
5400 KOLENZ, GERMANY

2 DEFENSE RESEARCH ESTABLISHMENT
SUFFIELD
ATTN: D. RITZEL
TECH LIB
PO BOX 4000
MEDICINE HAT
ALBERTA, T1A 8K6 CANADA

4 DSTO, MATERIALS RESEARCH
LABORATORY
ATTN: N. BURMAN
D. SAUNDERS
M. BUCKLAND
TECH LIB
PO BOX 50
ASCOT VALE
VICTORIA, AUSTRALIA 3032

2 INDUSTRIEANLAGEN-
BETRIEBSGESGELLSCHAFT MBH
ATTN: TECH LIB
H. DIEKHOFF
ABTEILUNG FINITE
BERECHNUNGSVERFAHREN
EINSTEINSTRAβE 20, D-8012 OTTOBRUNN

8 MINISTRY OF DEFENSE
ATOMIC WEAPONS ESTABLISHMENT
ATTN: M. GERMAN
J. THREAGOLD
W. BABBAGE
B. BOGARTZ
I. SMITH
J. TATE
M. KING
TECH LIB
FOULNESS, ESSEX, SS3 9XE, UK

NO. OF COPIES ORGANIZATION

4 MINISTRE DE LA DEFENSE
CENTRE D'ETUDE DE GRAMAT
ATTN: S. GRATIAS
E. CANTON
D. MERGNAT
TECH LIB
46500 GRAMAT, FRANCE

2 MINISTERE DE L'EQUIPMENT
LABORATOIRE D'ESSAIS D'EQUIPEMENTS
D'ABRIS
ATTN: TECH LIB
D. FAU
BASE DE VIROULOU-ALVIGNAC
46500 GRAMAT, FRANCE

2 NATIONAL DEFENSE RESEARCH INSTITUTE
WEAPONS TECHNOLOGY DEPARTMENT
ATTN: H. AXELSSON
TECH LIB
PO BOX 98
S-147 00 TUMBA, SWEDEN

2 NORWEGIAN DEFENSE CONSTRUCTION SERVICE
TEST AND DEVELOPMENT SECTION
ATTN: TECH LIB
A. JENSSEN
OSLO MIL/AKERSHUS
OSLO, NORWAY

3 STORES AND CLOTHING RESEARCH AND
DEVELOPMENT ESTABLISHMENT
ATTN: S. ELTON
S. CROSS
TECH LIB
FLAGSTAFF RD
ESSEX, CO2 7SS, UK

3 WEHRWISSENSCHAFTLICHE DIENSTELLE FÜR
SPRENGMITTEL UND SONDERTECHNIK
ATTN: M. KLAUS
L. KLUBERT
TECH LIB
OBERJETTENBERG
8230 SCHNIZLREUTH, GERMANY

NO. OF COPIES	ORGANIZATION
2	WEHRWISSENSCHAFTLICHE DIENSTELLE DER BUNDESWEHR FÜR ABC-SCHUTZ ATTN: W. REHMANN TECH LIB HUMBOLTSTRAβE/POSTFACH 1142 3042 MÜNSTER, GERMANY
1	DEWEY MCMILLAN & ASSOCIATES, INC. ATTN: J. DEWEY 1741 FELTHAM RD VICTORIA, BC V8N 2A4, CANADA

USER EVALUATION SHEET/CHANGE OF ADDRESS

This Laboratory undertakes a continuing effort to improve the quality of the reports it publishes. Your comments/answers to the items/questions below will aid us in our efforts.

1. ARL Report Number ARL-TR-784 Date of Report June 1995

2. Date Report Received _____

3. Does this report satisfy a need? (Comment on purpose, related project, or other area of interest for which the report will be used.) _____

_____

_____

4. Specifically, how is the report being used? (Information source, design data, procedure, source of ideas, etc.)

_____

_____

_____

5. Has the information in this report led to any quantitative savings as far as man-hours or dollars saved, operating costs avoided, or efficiencies achieved, etc? If so, please elaborate. _____

_____

_____

6. General Comments. What do you think should be changed to improve future reports? (Indicate changes to organization, technical content, format, etc.) _____

_____

_____

_____

CURRENT ADDRESS

_____
Organization

_____
Name

_____
Street or P.O. Box No.

_____
City, State, Zip Code

7. If indicating a Change of Address or Address Correction, please provide the Current or Correct address above and the Old or Incorrect address below.

OLD ADDRESS

_____
Organization

_____
Name

_____
Street or P.O. Box No.

_____
City, State, Zip Code

(Remove this sheet, fold as indicated, tape closed, and mail.)
(DO NOT STAPLE)